

LA--9511-C

DE83 008275

LA-9511-C
Conference

UC-28
Issued: January 1983

Proceedings of the Workshop on LAMPF II Synchrotron

**February 8-12, 1982
Los Alamos, New Mexico**

**Compiled by
R. K. Cooper**

DISCLAIMER

This report was prepared as an account of work sponsored by an agency of the United States Government. Neither the United States Government nor any agency thereof, nor any of their employees, makes any warranty, express or implied, or assumes any legal liability or responsibility for the accuracy, completeness, or usefulness of any information, apparatus, product, or process disclosed, or represents that its use would not infringe privately owned rights. Reference herein to any specific commercial product, process, or service by trade name, trademark, manufacturer, or otherwise does not necessarily constitute or imply its endorsement, recommendation, or favoring by the United States Government or any agency thereof. The views and opinions of authors expressed herein do not necessarily state or reflect those of the United States Government or any agency thereof.

NOTICE

PORTIONS OF THIS REPORT ARE ILLEGIBLE. It
has been reproduced from the best available
copy to permit the broadest possible avail-
ability.

Los Alamos Los Alamos National Laboratory
Los Alamos, New Mexico 87545

11. *Leptodora* sp. (1970)

CONTENTS

WORKSHOP SUMMARY by Richard K. Cooper	vii
PARAMETERS LIST	viii
ABSTRACT	1
CONSIDERATIONS FOR A STAGED APPROACH TO SYNCHROTRON CONSTRUCTION by L. Teng, L. Smith, and M. Barton	2
CONSIDERATION OF ENERGY AND COST FOR A KAON AND/OR p FACTORY by F. R. Huson	6
CHANGING THE TRANSITION ENERGY IN THE MAIN RING, FERMILAB p NOTE NO. 105 by S. Ohnuma	13
LATTICE WITH 50% UNDISPERSED STRAIGHT SECTIONS by J. Staples and A. Thiessen	26
BUNCH WIDTH CONSIDERATIONS IN A STRETCHER RING by M. Q. Barton	27
A SELF-CONSISTENT LONGITUDINAL DISTRIBUTION by L. Smith	31
RAPID-CYCLING TUNED rf CAVITY FOR SYNCHROTRON USE by D. A. Swenson and J. M. Potter	36
CONSIDERATIONS ON A HIGH-SHUNT IMPEDANCE TUNABLE rf CAVITY by P. L. Morton	38
ROTATING CONDENSERS by M. Foss	43

LOW EXTRACTION FROM THE STRETCHER RING by J. Staples	47
AN ANTIPROTON SOURCE FOR LAMPF-II by J. Simpson	49
SYNCHROTRON MAGNET CIRCUIT by M. Foss	58
POWER SUPPLY AND RING MAGNET OPTIONS by W. Praeg	65
NOTES FOR A KAON FACTORY DESIGN by G. H. Rees, R. K. Cooper	77

WORKSHOP SUMMARY
Richard K. Cooper

The LAMPF-II Synchrotron Workshop was convened to consider how one could provide physics experimenters with a high-intensity 16-GeV proton beam. The tentative parameters set by the experimenters were 16 GeV, 100 μ A, essentially continuous beam consisting of subnanosecond pulses separated by 20 ns. To provide the continuous beam a stretcher ring was envisioned, fed by a rapid cycling synchrotron. The parameter list included in these proceedings gives an idea of the possible variants on this basic scheme.

Before coming to the Workshop, the participants received the incomplete "Notes for a Kaon Factory Design," which is included as the final paper in these proceedings. The Workshop participants from laboratories other than Los Alamos were

Mark Barton, BNL
Martyn Foss, ANL
Alper Garren, LBL
Russell Huson, FNAL
Philip Morton, SLAC
James Simpson, ANL
Lloyd Smith, LBL
John Staples, LBL
Lee Teng, FNAL

As usual, participation in the Workshop does not necessarily constitute endorsement of the project.

PARAMETER LIST

	Accumulator	Booster	Synchrotron	Stretcher
E_0	800 MeV	0.8	4	16
E_{final}	800 ⁺ MeV	4 MeV	16	16
R	142 m	142	142	142
	DC ring for injection mech. (don't worry about resonance supply) supply)			
Repetition rate	dc	60 Hz	60 Hz	dc
Extraction	Single turn	Single turn	Single turn	Resonant
Injection	H ⁻ stripping	Single turn	Single turn	Single turn
Charges/bunch	10^{13} /bunch $5 \cdot 10^8$ /pulse 10^5 pulse/Mpulse 201.25 MHz	10^{13}	10^{13}	10^{13} /bunch
rf frequency	40	40.25 + x	x + 48	332.3
h	142'	142	142	7 x 142
$\frac{\Delta E}{\Delta \phi_{rev}}$	0.5-0.1 eV • s/bunch	0.5-0.1 eV • s/bunch	0.5-0.1 eV • s/bunch	0.5-0.1 eV • s/bunch
Total bunch length at extraction	?	?	1 ns	0.5 ns
$\epsilon_{x,y} = 10 \text{ \mu rad} \cdot \text{m}$				

PROCEEDINGS OF THE
WORKSHOP ON LAMPF II SYNCHROTRON

February 8-12, 1982
Los Alamos, New Mexico

Compiled by
R. K. Cooper

ABSTRACT

The Workshop on LAMPF II Synchrotron was held in Los Alamos, New Mexico, February 8-12, 1982. This publication contains the texts of the invited and contributed papers.

CONSIDERATIONS FOR A STAGED APPROACH
TO SYNCHROTRON CONSTRUCTION

by

L. Teng, L. Smith, and M. Barton

In defining and scoping the project we encountered at the very outset the usual dilemma. On the one hand the project must be sufficiently exciting and capable of supporting a broad area of challenging physics research so as to arouse the necessary interest and support of a large community of users. On the other hand the budget must be kept within reason and proportionate to available funds so that there is reasonable chance of gaining approval by the funding agency. For the proposal to be successful, one must strike a compromise between these two desires.

A strong case has been made by the physics community that the ultimate capability of the facility should be in the range of 16-GeV beam energy and $100-\mu\text{A}$ beam current. While such an ultimate goal is certainly within present day technology, several operational requirements are outside existing experience, the most prominent being the handling of the large amount of induced radioactivity. Thus, a staged approach to the construction in which the experiences gained at one stage can be used in the design of the succeeding stage may very well lead to a lower overall cost and, more important, a better ultimate facility. Such a staged approach, if properly composed, could also reduce the requisite rate of funding without significantly delaying the schedule for attaining the ultimate performance goal.

Many different staged approaches were suggested. We list them below and discuss their individual merits and drawbacks. The evaluation is based on the consideration of the following issues:

1. The capability for interesting physics research at each stage.
2. The projected schedule of completion of the stages.
3. The availability or interruption of the facility for physics at each stage while the next stage of construction is in progress.

4. The reliability of operation of each stage, especially of the final stage.
5. The total cost to reach the ultimate performance goal.
6. The requisite funding and expenditure rate. This may well be more important than the total cost.
7. The required design and construction expertise and manpower, especially in relation to those available at the present and as projected in the future.

It should be pointed out that some components of the accelerator complex lend themselves naturally to a staged approach. These are the experimental areas and facilities, the spill stretcher ring, and perhaps also the accumulator ring for injection. It would surprise no one to start the initial operation of the synchrotron with no stretcher or accumulator ring and only a skeletal experimental area. These items are then added as a matter of course to improve the performance and the use of the facility. In this category we can also include such longer range extensions of capabilities as deuteron acceleration, polarized beams, etc. The staged approach considered here refers only to the design and construction of the synchrotron proper. For each staged approach listed below comparison is made on the issues mentioned above relative to the reference case of a single stage to the final goal of 16 GeV and 100 μ A.

APPROACH A The Two-ring Scheme: 4-GeV Booster as First Stage Injecting into a 16-GeV Main Synchrotron as Second Stage.

Several variants of this theme were discussed. The rings could be in separate tunnels and thereby could have grossly different circumferences, or they could have roughly equal circumferences and hence could be installed in the same tunnel. For either arrangement we detect the following failings. First, the stages are too independent, so that the repeated process of proposal submission, review, authorization, and appropriation for the main synchrotron will undoubtedly make the total schedule rather long. The time to the ultimate performance goal may very well be double that of a single staged approach. Second, although the necessary funding rate is reduced by such a

two-stage approach, the total cost is certainly higher, and likely by a large amount, than that of the single stage. Third, and most important, the utility of a 4-GeV proton machine for physics is questionable. Some users did indeed express interest in such a facility. Nevertheless, the fact remains that many proton synchrotrons of similar and higher energies--Cosmotron and PPA at 3 GeV, Bevatron at 6 GeV, ZGS at 12 GeV--have been shut down. The saleability of a 4-GeV machine, high intensity or not, is not good. Fourth, the two-synchrotron complex at 16 GeV will be more complex to operate and less reliable than a single 16-GeV synchrotron. Finally, if there is any overlap in time in the execution of these two rings, the demand of expertise and manpower will be greater than that for the single stage.

APPROACH B The Inverted Two-ring Scheme: A 16-GeV Ring with Small Aperture, Hence Low Intensity as First Stage, A Booster of ~4-GeV added in Second Stage to Reach the Ultimate Intensity Goal.

This reverse strategy reduces but does not totally eliminate the objections mentioned for Approach A above. The first stage provides only a low (or normal) intensity 16-GeV machine. The utility of such a machine for physics is questionable at best, in view of the existing normal intensity 30-GeV AGS and 28-GeV CPS. Although much less likely, it nevertheless is conceivable that the second stage, which will have to be submitted as an independent construction proposal, is not approved. The total cost is still high and the overall schedule still protracted.

APPROACH C The Missing Magnet Scheme: In Stage One the Main Synchrotron is Built But Without, Say, Half the Dipoles, Hence Limited to Half Energy: The Missing Magnets are Added in Stage Two.

In addition to being technically awkward several component systems (magnet power supply, cooling, vacuum, beam monitor, correction magnet, etc.) must be redone in stage two. Most important, the differential in cost between such a stage one and the full single stage machine is rather small. Little of the advantage of a staged approach, particularly a lower funding rate, is gained by this missing-magnet approach. The start-up and operation of a synchrotron with missing dipoles also tend to be more difficult.

APPROACH D The Missing-rf (Perhaps, also magnet power supply) Scheme: Full Ring but Reduced rf, Hence Reduced Energy and Intensity, As Stage One; More rf is Added in Successive Stages Until Full Performance is Reached.

The rf system is the most costly single component system. It can amount to 30% of the cost of the synchrotron proper. Thus, the cost of the synchrotron and the necessary funding rate can be substantially reduced by reducing the rf system. The required rf voltage per turn is proportional to the peak energy and to the magnet cycling rate. For example, 2-GeV peak energy at full cycle rate requires only 1/8 the rf system for 16 GeV. The addition of rf is a continuous staging progression which can be absorbed by operating funds. Experiences in reducing beam loss and in coping with induced radioactivity can be gained at lower energy and intensity. Each step of increase in energy and intensity can be scheduled whenever one feels ready to battle the next higher level of radioactivity and the size of the step can be adjusted appropriately. There is no increase in total cost from that of the standard single stage machine. The rate of expenditure, insofar as the 30% for the rf system is concerned can be reduced to whatever required. There is no added complication in operation and reliability at each stage and the finished final machine is exactly the same as the single stage machine except for the modifications and improvements which may have been added from the experiences gained along the way of this staged approach. For these reasons we consider this approach of continuous staging the most effective and appealing.

CONSIDERATION OF ENERGY AND COST FOR
A KAON AND/OR \bar{p} FACTORY

by

F. R. Huson

There have been many studies of high intensity synchrotrons for producing kaons and \bar{p} 's. Some recent papers are listed in Ref. 1. In this note I will consider the requirements for the accelerator and very approximate cost estimates for three alternative designs; (1) a minimum cost accelerator for kaons, (2) a more flexible--larger radius accelerator for kaons, and (3) a minimum cost accelerator for p 's and kaons. This will provide information on fixed energy vs radius costs and energy with maximum radius vs cost.

Desirable features that most physicists agree on are

1. $\geq 1 \times 10^{14}$ protons per second (10X improvement). This requires rapid cycling (>10 Hz).
2. $\geq 90\%$ macroduty factor (2X improvement). This requires a dc storage ring.
3. \leq nanosecond and 50-100 MHz substructure for time of flight measurements. This requires a special lattice (see attached paper by Sho Ohnuma).

The consideration of energy is a more difficult choice. Figures 1 and 2 present the invariant cross section vs energy curves. The conclusions are

Particles	Minimum Momentum for \sim Maximum Production	Minimum Momentum for 1/2 Maximum Production
K^+, Σ^-, Λ	15 GeV/c	7 GeV/c
K^-, Ξ^+	23	15
\bar{p}	80	45

In my opinion, there are two momenta to consider; (1) ≥ 15 GeV/c for kaon and hyperon physics, and (2) ≥ 45 GeV/c for kaon, hyperon and \bar{p} physics. We assume that the cycle time would be proportional to the energy, thus the gain in invariant cross section versus energy is compensated by cycle time in the

Figure 1a. Invariant kaon production σ at maximum production momentum (p momentum marked on curves by arrows). Note invariant cross section is plotted since the number of secondaries per unit time is approximately proportional to the invariant differential cross section.

$$\frac{dN}{dt} = \left(\frac{E}{dp} \right) \left(\frac{p \Delta p \Delta \Omega}{\sigma t} \right)$$

$$\left(\frac{p \Delta p \Delta \Omega}{\sigma t} \right) \approx \frac{p \Delta \Omega \pi p^2}{\sigma t p^2} = \frac{\pi}{\sigma t} \left(\frac{\Delta p}{p} \right) p^2 \approx \text{constant}$$

Note the different threshold behavior for K^+ (only additional $s\bar{s}$ quarks needed) and K^- (additional $u\bar{u} + s\bar{s}$ quarks required). Points on the right side of graph are for 200 GeV/c.

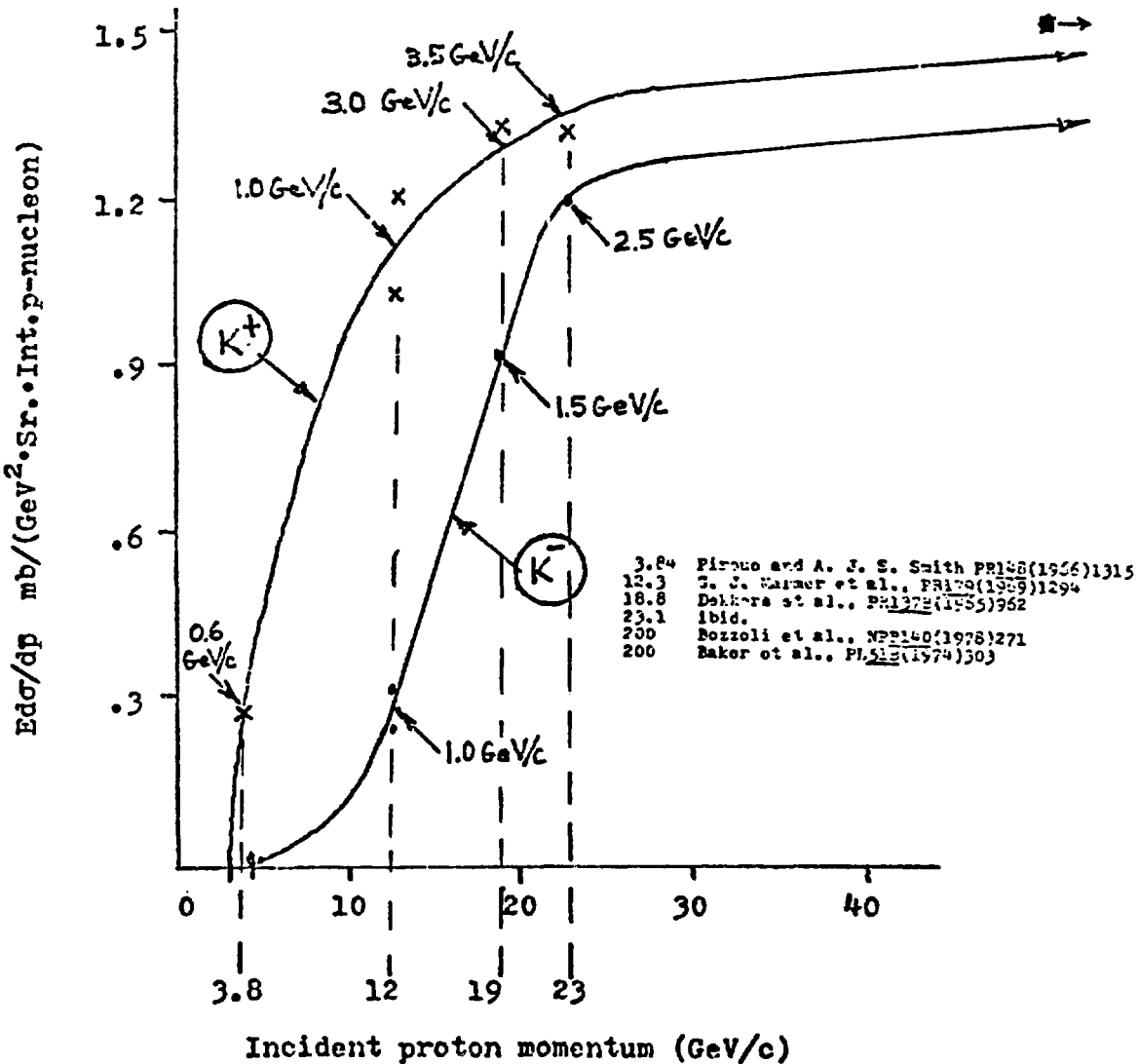


Figure 1b. Invariant \bar{p} production σ from $p p$ (H) and $p + Pb$ at maximum production momentum (p momentum marked on curve by arrows). A dependence is assumed to be $A^{2/3}$. Note \bar{p} production requires an additional $2u\bar{u} + d\bar{d}$ quarks.

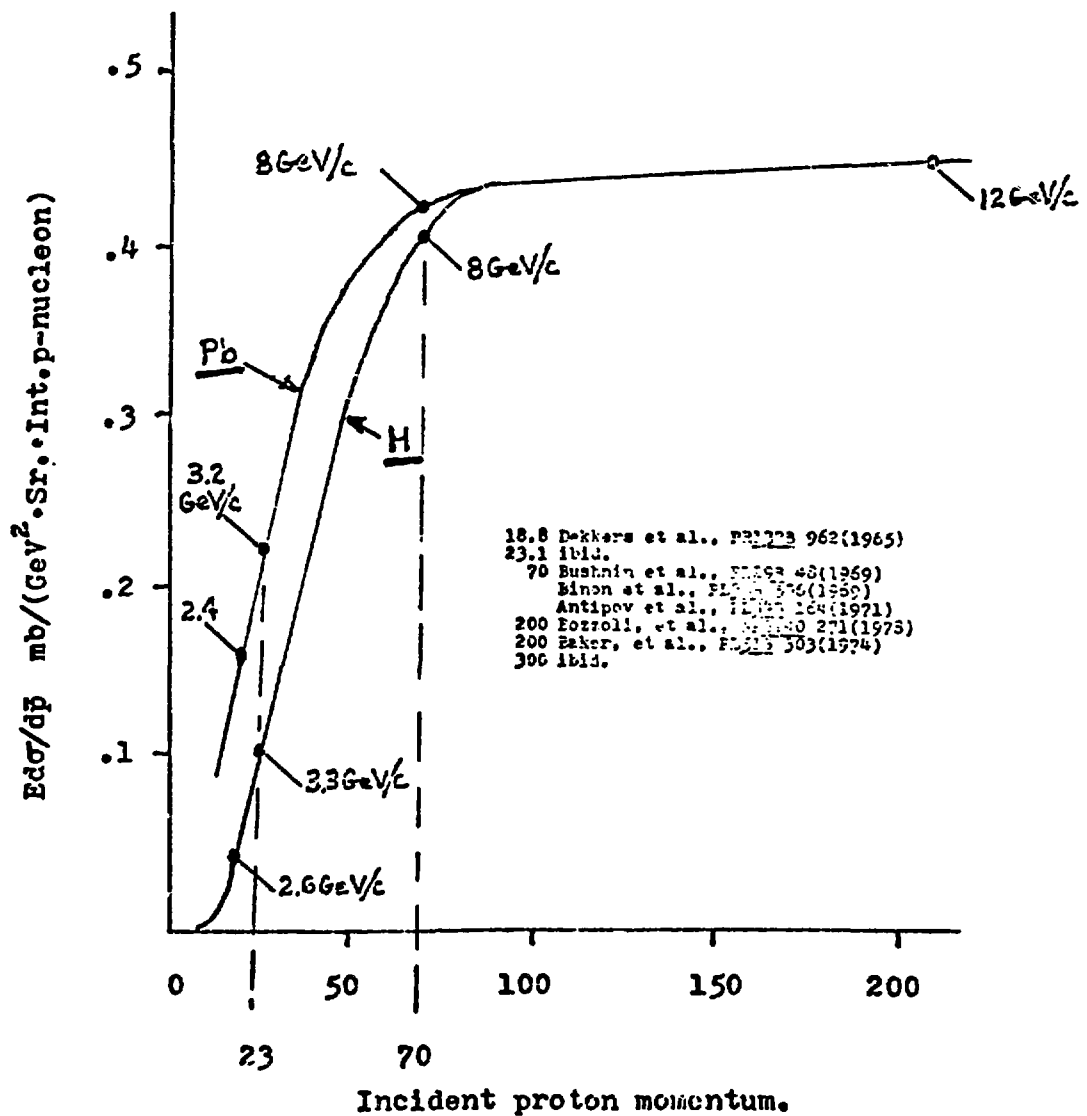
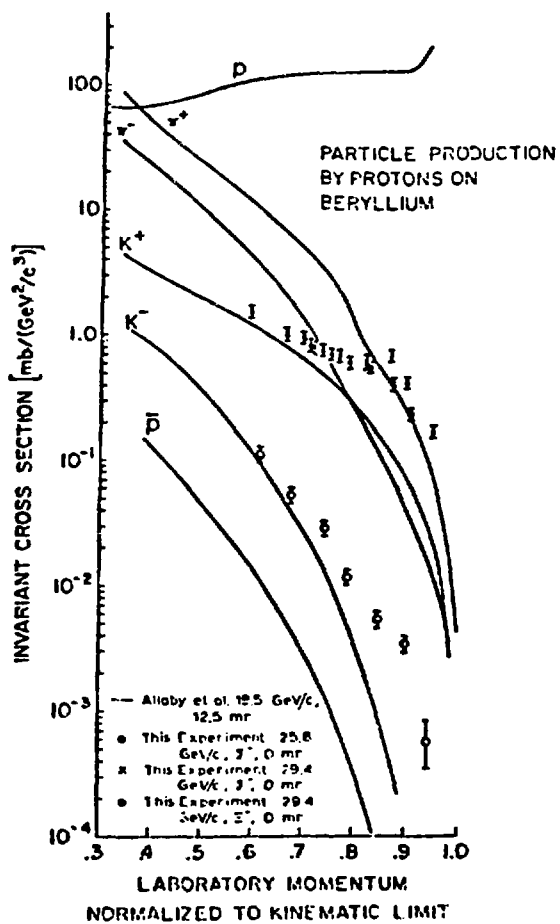


Figure 2. This figure is reproduced from V. Hungerbühler et al., PRD12(1975)1203. Note Σ^- production follows K^+ and Ξ^- production K^- as would be expected from quark arguments.



limited energy range we are considering. We note that the \bar{p} production and collection is limited by cooling time (see J. Simpson's report), thus the high intensity, via rapid cycling, only helps if multiple cooling rings (>10) are used. (This is the only solution known at this time; future innovation is clearly needed).

Cost estimates are very much a function of the people responsible for the construction. The style of construction can change the cost as much as a factor of 2. I will attempt to present a minimum cost. The cost is based on the machine in Ref. 1, "A Regional Facility". The other machines are then scaled from that machine by the scaling laws in the table.

TABLE I

TOTAL COST OF ACCELERATORS^a

	15 GeV/c	15 GeV/c	45 GeV/c
	<u>R = 51 m</u>	<u>R = 133 m</u>	<u>R = 153 m</u>
	<u>f = 30 Hz</u>	<u>f = 30 Hz</u>	<u>f = 10 Hz</u>
Booster	12 000	21 592	19 854
Storage Ring	8 200	13 915	19 532
Buildings	6 000	10 988	12 928
Salaries	<u>8 800</u>	<u>8 800</u>	<u>15 242</u>
Total	35 000	55 295	67 556

^aCosts do not include an 800-MeV injector, experimental areas, overhead, contingency and inflation. These would more than double the costs.

Whereas the cost estimates presented are approximate they do scale from the Fermilab booster (adding \$6 million to rf for ferrite problems to take β from 0.57 to ~ 0.99) to the Fermilab main ring. My conclusions are that the radius of the accelerator should be minimized. It appears to me that 15 GeV/c with 50 m radius is near minimum. By the time everything is included this will be at least a \$75 million project.

REFERENCES

1. R. R. Wilson, A Staged 2- to 20-GeV Proton Synchrotron, August 1980
L. C. Teng, A High Intensity Accelerator Facility, LA-8775-C, 1981
G. H. Rees and R. K. Cooper, Notes for a Kaon Factory Design, LAMPF II
Workshop, February 1982.
F. R. Huson, A Regional Accelerator Project, Pan American Symposium on
Elementary Particles and Technology, Cocayoc Mexico, January 5-7, 1982.
2. S. Ohnuma, "Changing the Transition Energy in the Main Ring", p Note No.
105 Fermilab, December 1980.

<u>Components</u>	<u>Cost</u>		<u>COST \$K</u> <u>RCB</u>			<u>SR</u>		
	E = Const, R varies	vary E/R	15 GeV/c R = 51 m f = 30 Hz	15 GeV/c R = 133 f = 30 Hz	45 GeV/c R = 153 f = 10 Hz	15 GeV/c P. = 51	15 GeV/c R = 133	45 GeV/c R = 153 m
Dipoles	Const.	E	1200	1200	3600	900	900	2700
Quads	R	E	550	1434	1650	700	1825	2100
Vac	R	R	400	1043	1200	600	1565	1800
Power Supply	Const.	Ef	2000	2000	2000	500	500	1500
rf*	R	Rf	4000	10431	4000	1000*	2608	3000
Spec. eq.	R	R	500	1304	1500	500	1304	1500
Inj + ext	Const.	✓E	1000	1000	1732	1500	1500	2600
Controls	Const.	✓E	1000	1000	1732	500+	1000	866
Refrigeration	R 1/4	✓E				1500	1906	2600
Misc.	✓R	4✓RE	<u>1350</u>	<u>2180</u>	<u>2340</u>	<u>500+</u>	<u>807</u>	<u>1866</u>
Total			12 000	21 592	19 854	8200	13 915	19 532
<u>Buildings</u>								
Tunnel	R	R	2000	5216	6000	-†		
Access & Galleries	✓R	✓R	2000	3230	3464	-†		
Building & Util.	R 1/4	R 1/4 E 1/4	2000 6000	2542 10 988	3464 12 928	-†		
<u>Salaries</u>	Const.	✓E	8800	8800	15 242	-†		

*The rf costs would increase considerably if a bunch less than 1 nanoseconds were required.

†Assumes storage ring uses part of rapid cycling booster equipment.



Fermilab

P Note No. 105
December 5, 1980

Changing the Transition Energy in the Main Ring

S. Ohnuma

December 5, 1980

I.

Regardless of what we do to collect and cool the \bar{p} beam, it is almost always better to start with a small value of the initial longitudinal phase space area. If the longitudinal emittance is fixed to a certain value, we gain in the number of \bar{p} 's by taking a larger bite of $\Delta p/p$ and a correspondingly smaller bunch length as long as the transport system after the target can handle the momentum spread and the precooler can contain the beam stably during the time the momentum spread is getting reduced by, for example, bunch rotation. Since the bunch length of \bar{p} is essentially that of the proton bunches extracted from the main ring, it is desirable to make this length as short as possible in the main ring at the time of extraction, that is, at around 80 to 100 GeV. The most straightforward method for this is to change the transition energy of the main ring from the normal value of $\gamma_t = 18.75$ (kinetic energy 16.6 GeV) to a value near the extraction energy. Following examples will clearly illustrate the point. It is assumed here that the rf is stationary (no energy gain) when proton bunches are extracted.

stationary bucket area A (in eV-s)

$$A = 0.0181 \times (E \cdot V / |n|)^{1/2}$$

where the total energy E ($\equiv m_p c^2 \gamma$) is in GeV, the peak rf voltage V

is in MV and

$$\eta \equiv 1/\gamma_t^2 - 1/\gamma^2$$

bucket half height in $(\Delta p/p)$

$$(\Delta p/p)_{\text{bucket}} = \pm 0.756 \times 10^{-3} (V/E \cdot |\eta|)^{1/2}$$

When the bunch area is S eV-s, the bunch length $2\phi_B$ (in rad.) is

$$2\phi_B \approx 8 \cdot (S/\pi A)^{1/2}$$

The error of this expression for ϕ_B is less than 1% for $\phi_B < 30^\circ$.

The momentum spread (half) of the bunch is

$$(\Delta p/p)_{\text{bunch}} = (\Delta p/p)_{\text{bucket}} \cdot \sin(\phi_B/2)$$

This expression is exact when the exact value of ϕ_B is used.

1. $\gamma_t = 18.75$, normal main ring lattice

Take $E = 100$, $V = 4$, $S = 0.2$.

$$\eta = 0.002756, \quad A = 6.9 \text{ eV-s}, \quad (\Delta p/p)_{\text{bucket}} = \pm 2.88 \times 10^{-3}$$

$$\phi_B = \pm 22^\circ \text{ (2.3 ns full)}, \quad (\Delta p/p)_{\text{bunch}} = \pm 0.55 \times 10^{-3}$$

2. $\gamma_t = 60$, all other parameters the same as for 1. above.

$$\eta = 0.0001897, \quad A = 26.3 \text{ eV-s}, \quad (\Delta p/p)_{\text{bucket}} = \pm 1.10 \times 10^{-2}$$

$$\phi_B = \pm 11.3^\circ \text{ (1.2 ns full)}, \quad (\Delta p/p)_{\text{bunch}} = \pm 1.08 \times 10^{-3}$$

By further increasing the value of γ_t , we may decrease the bunch length to even smaller values but there is a limit to this reduction. Near the transition energy, the adiabatic approximation used to derive the

above expression for rf bucket is not really valid and a better procedure is necessary to estimate the correct bunch shape.* The bunch length takes its minimum value at $\gamma = \gamma_t$,

$$\text{min. } \phi_B \text{ (in rad.)} = 9.03 (\gamma_t)^{-2/3} S^{1/2} \left(\frac{\tan^2 \phi_s}{\dot{E}} \right)^{1/6}$$

where $\dot{E} \equiv dE/dt$ is in GeV/sec, S is in ev-s and the synchronous phase angle ϕ_s is determined by the relation

$$eV \sin \phi_s \text{ (in MeV)} = 0.0210 \dot{E} \text{ (in GeV/sec)}$$

The momentum spread (half) takes its maximum value

$$\text{max. } (\Delta p/p)_{\text{bunch}} = 0.123 \left(\frac{S}{E \cdot \text{min. } \phi_B} \right)$$

The bunch shape is not an ellipse and the value of $(\Delta p/p)$ is larger by a factor of $2/\sqrt{3}$ compared to an elliptic shape of the same area. If we take $\dot{E} = 100$ GeV/sec and $V = 3$ MV at $\gamma = \gamma_t$,

$$\phi_s = 44.4^\circ,$$

$$\text{min. } \phi_B = 15.1^\circ \text{ (1.6 ns full) for } \gamma_t = 18.75,$$

$$= 7.0^\circ \text{ (.73 ns full) for } \gamma_t = 60,$$

$$(\Delta p/p) = \pm 0.93 \times 10^{-3} \text{ for } \gamma_t = 18.75,$$

$$= \pm 2.02 \times 10^{-3} \text{ for } \gamma_t = 60.$$

There is a characteristic time interval T such that the adiabatic picture of rf bucket (and the bunch shape) is not valid within a few times T measured from the transition crossing. For the main ring,

$$T \text{ (in ms)} = 1.10 \times (\gamma_t^4 \cdot \tan \phi_s / \dot{E}^2)^{1/3},$$

$$T = 2.5 \text{ ms } (\gamma_t = 18.75) \text{ and } 12 \text{ ms } (\gamma_t = 60).$$

* For this topic, see E. D. Courant, FN-187, May 20, 1969. Useful references are given there, mostly works by A. Sørensen of CERN.

Finally, it is interesting to note that the Sørensen parameter, which is a measure of the bunch area dilution in crossing the transition because of space charge, is independent of the value of γ_t .

II.

One might think that the easiest way to change the transition energy in the main ring is to increase the phase advance per cell. This is possible since the highest energy will be ~ 100 GeV instead of 400 GeV and the focal length of main quadrupoles can be made much shorter than the normal value of 26.0 m. However, this turns out to be a rather impractical method. Consider, for example, a ring made of 102 identical main ring normal cells. The maximum phase advance one can have is 180° per cell so that the maximum tune is 51. The transition energy does not increase as much, however, and the maximum value of β is prohibitive:

phase advance $174^\circ/\text{cell}$ (tune = 49.3)

$\gamma_t = 33.2$, $\beta_{\max} = 1,100$ m, $\beta_{\min} = 2.3$ m.

In the main ring, we have six superperiods with six long straights and six medium straights. When the phase advance per cell is increased by increasing the focal strength of main quadrupoles, the transition energy changes quite differently compared to the ring composed of γ normal cells only as one can see in the following table.

$(B'l/Bp)$	tune	γ_t	β_{\max}	range of x_p
$.060464 \text{ m}^{-1}$	35.185	35.082	271.6 m	-7.6 to 11.1 m
$.060544$	35.291	36.785	294.3	-9.8 to 13.4
$.060624$	35.404	40.145	328.9	-13.4 to 17.4
$.060663$	35.464	43.554	354.3	-16.3 to 20.5
$.060703$	35.529	50.768	389.8	-20.7 to 25.3

Since it is desirable to keep the tune constant from the injection to the extraction at ~ 100 GeV (one certainly cannot cross integer or half-integer resonances), one cannot avoid having large values of β_{\max} and the dispersion function x_p even at low energies where the transverse emittance and the momentum spread are both large. Besides, large values of β and of x_p are likely to be at the same location. For example, with tune = 35.404 (the third row),

station	β_{\max}	x_p
#13	303.5 m	-12.5 m
#28	296.3	15.6
#36	319.9	16.7
#44	329.9	17.4

Beyond $(B' l / B_p) = 0.060760 \text{ m}^{-1}$, the path length becomes shorter for a higher momentum particle and the transition energy is imaginary. It is questionable if this brute-force method would be useful in trying to reduce the bunch length.

III.

In the past, it was suggested that we should try a γ_t -jump (à la CERN PS) in the booster to reduce the space-charge mismatch (L. Teng, FN-207, April 17, 1970). A relatively simple system of twelve quadrupoles can change γ_t from 5.45 to 4.44. Later in 1978, Carlos Hojvat and I looked into this problem again in connection with the then proposed deceleration of \bar{p} in the booster. A fairly detailed design of a practical system has been worked out by Bruce Brown but nothing has come out of these efforts. It is unfortunate that most of these works remain as private memos unavailable for general use. For the main ring, I am not aware of any similar works done by other people.

Consider a system of trim quadrupoles placed in a ring. Using various formulas in Courant-Snyder, one can derive the following expression for the transition energy,

$$1/\gamma_t^2 = (1/\gamma_{t,0}^2) \cdot [1 + (9v^4/2\pi^2) \sum_{k>0} \frac{|J_k|^2}{(v^2 - k^2)(4v^2 - k^2)^2}]$$

where $\gamma_{t,0}$ is the unperturbed value of γ and

$$J_k = \sum_i \beta_i (B' \lambda / B_0)_i e^{-ik\phi_i}$$

Here the summation is over all trim quadrupoles and ϕ_i is the normalized phase (phase/tune) at the i -th trim quadrupole. This expression has been very useful in designing the quadrupole system for γ_t -jump in the booster. For example, when applied to the arrangement proposed by L. Teng with $|J_k| \neq 0$ for $k = 6, 18, 30, \dots$, the expression predicts a change of γ_t from the normal 5.446 to 4.14 (focal strength of 12 quadrupoles = 0.0304 m^{-1}) while the exact calculation gives 4.435. For another system with $|J_k| \neq 0$ for $k = 8, 16, 32, \dots$, the predicted value is 7.55 and the exact value is 7.494. In the main ring, we are interested in changing γ_t from the normal value of 18.75 to 40 or even higher. It is doubtful if this expression can be used for quantitative estimates of the required quadrupole strength but the following qualitative remarks should still be valid:

1. The component $k = 0$ does not affect γ but it changes the tune. It is important to make $J_0 = 0$ so that the tune remains the same at least in the lowest-order approximation.
2. Components with $k < v$ decrease the value of γ_t . If components with $k > v$ are dominant, γ_t increases and goes to imaginary values when the quantity within the square bracket becomes negative.
3. Of two factors in the denominator, the second, $(4v^2 - k^2)^2$, influences γ_t more than the first. One can change γ_t most easily by

making $|J_k|$ with $k \approx (2v)$ large. (Of course, this is not the case if one wants to decrease the value of γ_t .) The trouble with this is that the component J_k with k near $(2v)$ is precisely the one which is responsible for a large change in β , an unavoidable byproduct of γ_t change:

$$\frac{\Delta\beta}{\beta}(s) = - (v/\pi) \sum \frac{J_k e^{ik\phi(s)}}{4v^2 - k^2} \quad (\sum \text{ for } k = -\infty \text{ to } \infty)$$

Courant-Snyder, Eq. (4.53)

The best strategy is then to have a large $|J_k|$ at $k \approx v$ and all other $|J_k|$ as small as possible.

IV.

The first trim quadrupole system studied is composed of thirteen quadrupoles in each superperiod (total 78). They are all placed in ministraights, downstream of horizontally focusing main quadrupoles, but excited independently such that $\beta_i(B'l/Bp)_i$ follows $\cos(2l\phi)$. The arrangement is antisymmetric with the period three $(+-+-+-)$ so that $J_k \neq 0$ for $k = 3, 9, 15, \dots$. The unperturbed main ring has $v_x = 20.75$ and $v_y = 20.79$. These values can be kept fixed by a small amount of adjustment in the focal strength of main quadrupoles when the trim quadrupoles are excited to various levels. From the approximate expression for $1/\gamma_t^2$, one expects γ_t to become infinite at $\text{max.}(B'l/Bp) = 0.00274 \text{ m}^{-1}$ with only $J_{k=21}$. The exact value has been found to be 0.0049 m^{-1} (that is, $\text{max.}B'l = 16.4 \text{ kG}$ at 100 GeV/c). In Fig. 1, γ_t , $\text{max.}\beta_x$ and $\text{max.}X_p$ (dispersion function) are plotted as a function of $\text{max.}(B'l)$ at 100 GeV/c . For example, at $\text{max.}(B'l) = 13.4 \text{ kG}$, we have

$$\gamma_t = 64, \quad \text{max.}\beta_x = 203 \text{ m}, \quad \text{max.}X_p = 24 \text{ m}.$$

Combinations of β_x and x_p at various locations around the ring are not as bad as for the case given on p.5. For example,

station	β_x (m)	x_p (m)
A11	100	-18.2
A24	183	6.8
A26	48	24.0
B13	202	-8.5
B46	181	9.7

In operating this system for the extraction energy of 100 GeV, one would start exciting trim quadrupoles after the beam energy reached 80 GeV or so. Even then, the size of the beam coming from x_p is alarmingly large. Another system which is somewhat more realistic is shown in Fig. 2. There are six trim quadrupoles in each super-period but they are now all excited at the same strength. Obviously, the performance is not as attractive as the one shown in Fig. 1, especially because of large dispersions (max. $x_p = 31$ m for $\gamma_t = 40$).

A clever scheme for a γ_t -jump in the CERN PS (CPS) has been discussed by W. Hardt (Proceedings of the IXth International Conference on High Energy Accelerators, SLAC, May 1974, p. 434). and several people have asked me if we could employ a similar scheme in the booster. Hardt utilizes the fact that, in the CPS, the phase advance per cell is 45° (fixed since it is a combined-function machine) so that trim quadrupoles can be placed with phase intervals of 90° , 180° , etc. The system is composed of several doublets* with the phase advance of 180° between two elements of doublets. This choice of phase advance is beneficial in minimizing unwanted $|J_k|$ near $k = (2v)$ and also in reducing the higher-order effects of trim quadrupoles on the tune. In fact, it is not difficult to see (although Hardt does not use the same language) that the arrangement simply enhances one component J_k

*There are two triplets in the system but they can be regarded as four doublets. The strength of center quadrupole of a triplet is twice the strength of end quadrupoles and the polarity is reversed.

with $k = v$ suppressing, at the same time, J_k 's near $k = (2v)$. There are actually two independent systems so that all sorts of manipulations are possible, for example bunch-shape matching across the transition. However, for our present purpose, the essential point is to have an unperturbed ring with the phase advance of 45° or 90° per cell. Because of this requirement, it is difficult if not impossible to apply the idea in the booster.

As the unperturbed main ring, we may take the tune $v_x = 25.40$ with the focal strength of main quadrupoles increased to 0.0482 m^{-1} from the normal value of 0.0384 m^{-1} . The phase advance per regular cell is then very close to 90° . There are sixteen doublets in the ring arranged symmetrically,

sectors A and D : four doublets each with the relative strength of 1.

sectors B and E : four doublets each with the relative strength of 1.5

sectors C and F : none

The difference in the relative strength, 1 in A and D and 1.5 in B and E, is caused by the difference in β_x at quadrupole locations. The expected performance characteristics of this system are shown in Fig. 3. For example, with $B'l$ (relative strength 1) = 20.8 kG at 100 GeV/c, we have

$$Y_t = 60, \quad \text{max.} \beta_x = 203 \text{ m}, \quad \text{max.} |x_p| = 21.5 \text{ m.}$$

Note that the curve for $\text{max.} |x_p|$ breaks at $B'l = 16.8$ kG; the maximum magnitude of negative x_p exceeds that of positive x_p beyond this point. This system is probably superior in many respects to those in Figs. 1 and 2 provided the main ring can be operated stably at $v_x = 25.4$.

V.

The sole purpose of this note is to demonstrate that the transition energy of the main ring can be raised to any value without violating fundamental laws of physics. Most emphatically, it is never meant to be a proposal of practical systems for reducing the bunch length. Anyone can itemize dozens of problems that must be looked into carefully before such a system is considered seriously. I do not do so simply because I am afraid of missing some items. My only hope is that this note would be of some use to those who insist on pursuing the problem.

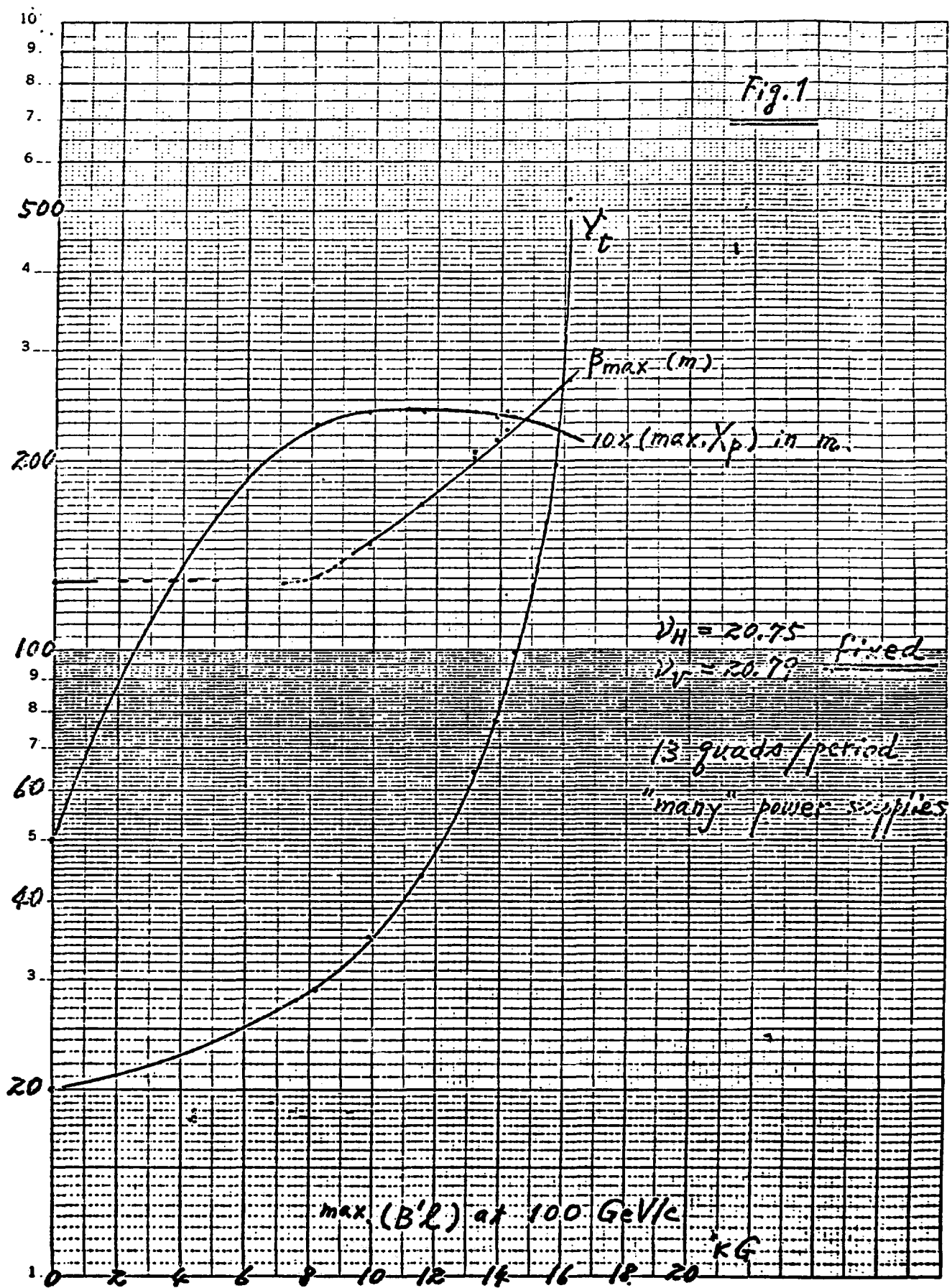
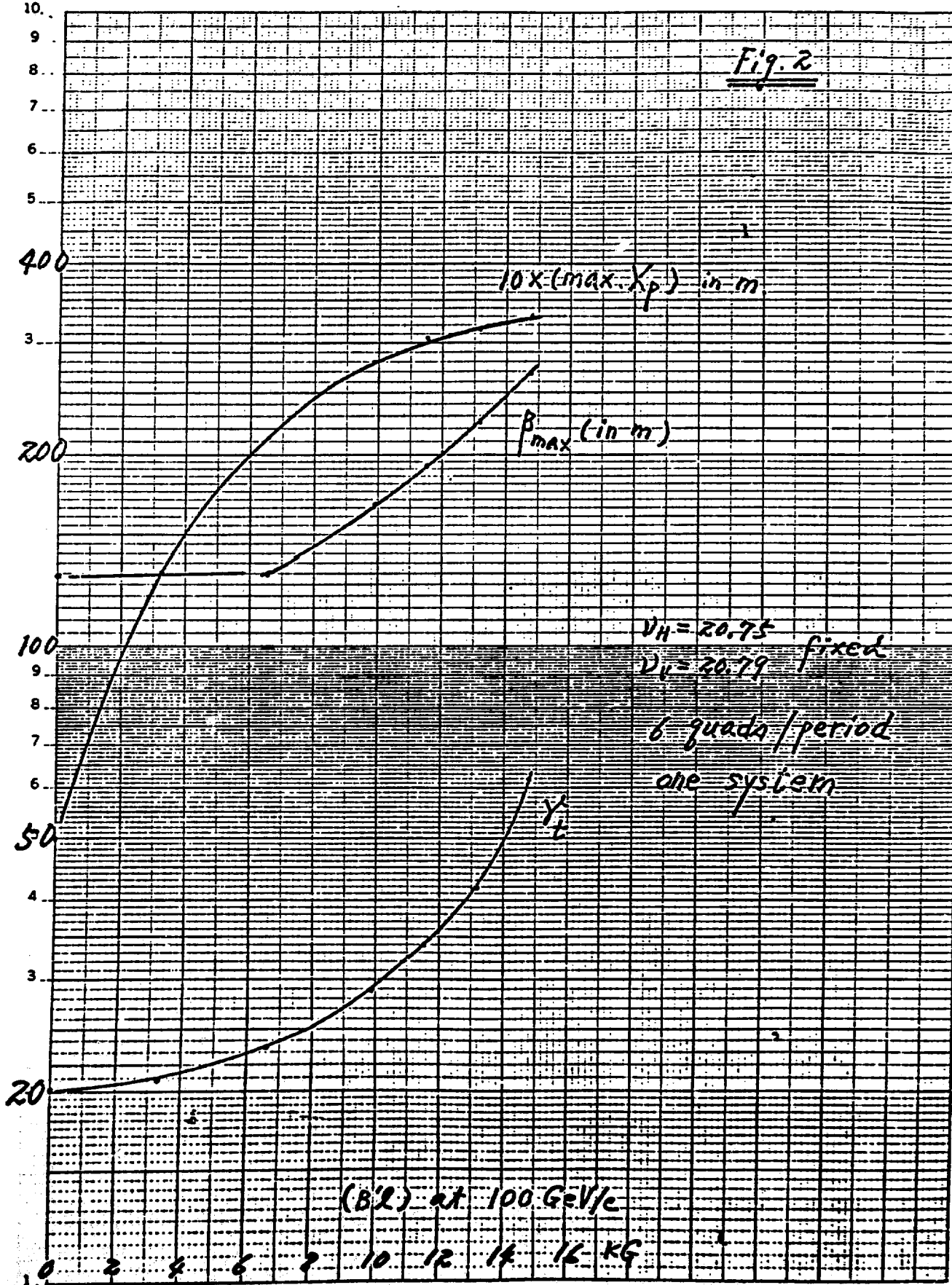
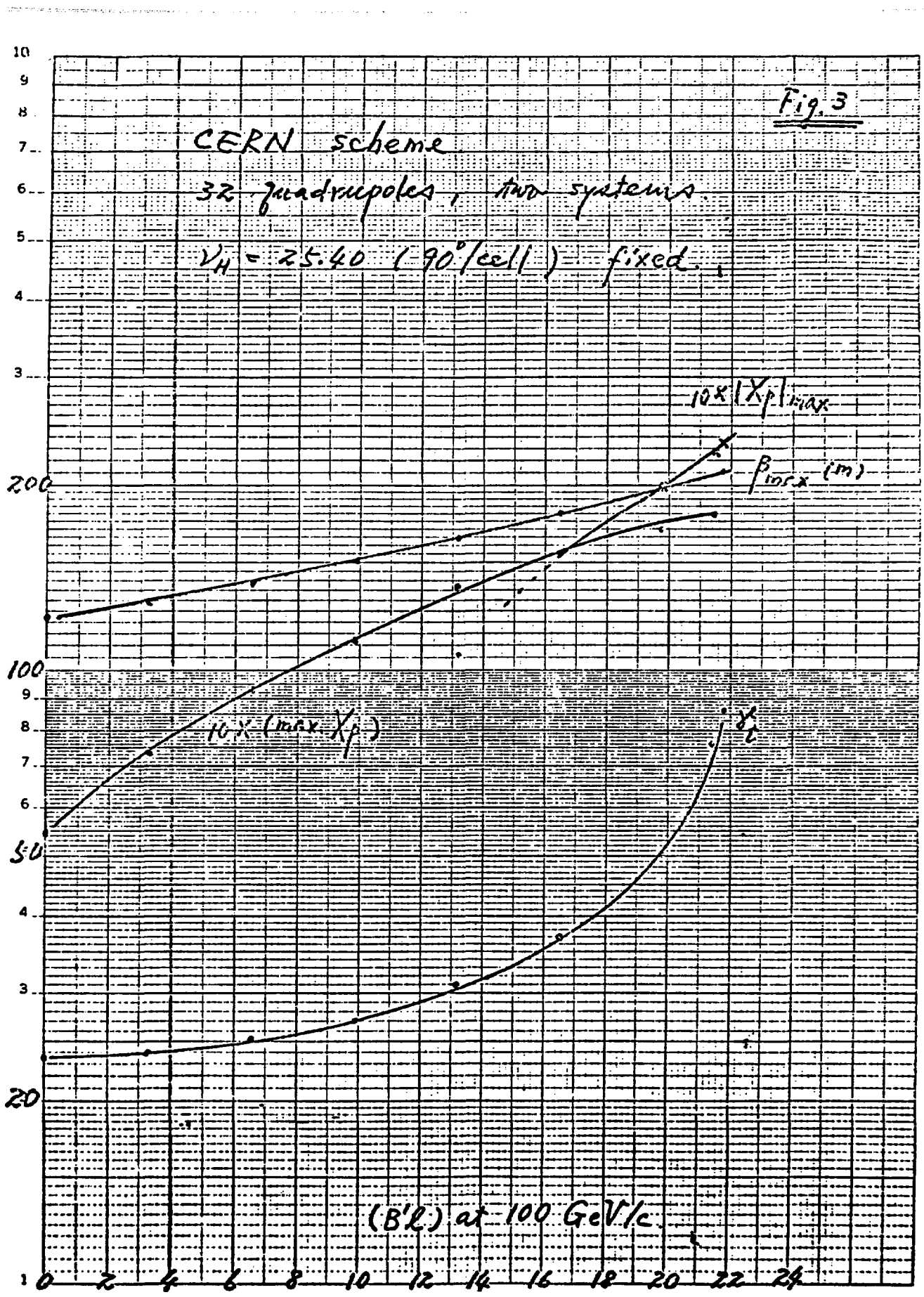


Fig. 2





LATTICE WITH 50% UNDISPERSED STRAIGHT SECTIONS

by

J. Staples and A. Thiessen

A lattice with 50%-empty, zero-dispersion cells is proposed. This very regular lattice consists of only two types of cells: a filled doublet cell with exactly $\pi/2$ phase advance and an empty doublet cell with slightly less than $\pi/2$ phase advance. The filled cells are grouped in fours, providing a naturally achromatic bend with a 2π phase advance.

The lattice investigated has the structure 12[4(FBD) (4F'OD')]. Twelve superperiods of 30° bend (four filled cells) are interposed with four empty cells. The total phase advance for one superperiod is $4\pi - \epsilon$, as the four empty cells contribute $2\pi - \epsilon$ to the superperiod. As the bend is automatically achromatic, it has a unity matrix except for a non-zero isochronicity term, which will set the transition energy. Thus the empty straight sections possess zero dispersion.

As well as having a large fraction of zero-dispersion straight sections, this has two other interesting properties. The geometric aberrations due to the dipole and sextupoles in the filled cells is cancelled due to symmetry, and the regularity of the lattice is very high due to the similarity of all cells.

For a lattice with a basic cell length of 8.8 m, 12 superperiods of the above described structure (total circumference of 844.8 m) $\beta_{x \text{ max}} = 13.2$ m, $\beta_{y \text{ max}} = 14.0$ m, and $n_{x \text{ max}} = 1.17$ m. Forty-eight straight sections, each 5.3 m long, are available; γ_t is 17.3 for the above-described lattice.

BUNCH WIDTH CONSIDERATIONS IN A STRETCHER RING

by

M. Q. BARTON

It is desirable to have a stretcher ring for the kaon factory to provide a usable macroscopic duty cycle. This ring would contain the beam in very tight bunches which would be resonantly extracted to provide a time structure suitable for time-of-flight experiments. It has been suggested that the choice of γ_t , the lattice transition gamma, close to the operating energy enhances the bunching for a given rf voltage. This argument is valid at low intensity but it may be simplistic at the current levels visualized for this project.

This can be seen from the rf "restoring force" $eV/2\pi(\cos \phi_s) h\phi$ where V is the peak rf voltage, ϕ_s is the synchronous phase (for a storage ring $\phi_s = 0$), h is the harmonic number, and ϕ the phase in units that go through 2π in the machine circumference. In the presence of "space charge", this becomes $(heV/2\pi-k)\phi$, where k arises from the longitudinal space charge. It is readily shown that

$$k = 3g\pi \left(\frac{r_0}{R}\right) \left(\frac{N}{h}\right) \frac{mc^2}{\gamma^2} \frac{1}{\phi_{\max}^3},$$

where $g = 1 + 2 \log (b/a)$ is a geometric factor describing the potential of a beam with unit charge per unit length, b is the chamber radius, and a the beam radius. The classical radius of the proton is r_0 and R is the major radius of the accelerator, (N/h) is the number of protons per bunch, mc^2 is the proton rest energy, γ is the usual relativistic factor, and ϕ_{\max} is the half width of the base of the bunch. This formula is derived on the assumption of a parabolic charge distribution that results in a linear longitudinal space charge force. This k is for the simple space charge. In general, the beam current excites voltage on various structures in the ring.

The ratio of these voltages to beam current is an impedance. The (Z/n) , where n is a harmonic number of the rotation frequency, is typically 10Ω for essentially all ring accelerators. The effective (Z/n) for our simple space charge is

$$\left(\frac{Z}{n}\right) = \frac{g}{2\gamma^2} Z_0 \quad ,$$

where Z_0 is the impedance of free space. At $\gamma = 18$, $g \sim 3$, this is about 2Ω . A more conservative approach is to let k be determined by the empirical Z/n :

$$k = 6 \left(\frac{Z}{n}\right) \cdot \frac{1}{Z_0} \pi \left(\frac{r_0}{R}\right) \left(\frac{N}{h}\right) mc^2 \frac{1}{\phi_{\max}^{3/2}}$$

and use $\sim 10 \Omega$ for (Z/n) .

From the equation of motions, one now finds the voltage required is

$$eV = \left[\frac{A^2 \ln \omega^2}{E \pi^2 \phi_{\max}^4} + k \right] \frac{2\pi}{h} \quad .$$

A is the bunch area in Volt-seconds, E is the energy, $\omega/2\pi$ is the rotation frequency, and η is $1/\gamma^2 - 1/\gamma_t^2$ where γ_t is the lattice transition γ .

A useful parameterization results if we allow the space charge term to be a fraction ρ of the rf restoring force. Then $k = \rho (heV/2\pi)$. Since $k \propto 1/\phi_{\max}^3$, ϕ_{\max} is determined. Then we can solve the voltage equation for η :

$$\eta = \left(\frac{heV}{2\pi}\right)^{-1/3} \left(\frac{1-\rho}{\rho^{4/3}}\right) \frac{E\pi^2 k^{4/3}}{A^2 \omega^2} \quad .$$

Using

$$\begin{aligned}Z/n &= 10\Omega, \\R &= 142 \text{ m}, \\N/h &= 1/142 \cdot 10^{13}, \\A &= 0.1 \text{ eV sec.}, \\E &= 16.938 \text{ GeV}, \\h &= 142,\end{aligned}$$

we can develop the following table for bunch width, $\Delta\tau$, and n versus ρ for the two cases $eV = 3 \text{ MeV/turn}$ and 10 MeV/turn .

TABLE I

<u>ρ</u>	3 MeV		10 MeV	
	<u>$\Delta\tau$ (ns)</u>	<u>n</u>	<u>$\Delta\tau$ (ns)</u>	<u>n</u>
0.01	7.7	1.09	5.15	0.73
0.03	5.3	0.24	3.55	0.166
0.1	3.57	0.046	2.39	0.031
0.3	2.48	0.0083	1.66	0.0056
1.0	1.66	0	1.11	0

What these numbers show is that, in any practical case, ρ will be large. One probably should not try to force $\Delta\tau$ to be very small by using a small n because that pushes ρ too high. The suggestion would be that a rather conventional n of ~ 0.01 should be chosen and one must be prepared to accept the high rf voltage required to obtain nanosecond bunch length. While the resulting bunch lengths may be larger than the experimenters desire, it should be pointed out that the resonant extraction process does sharpen the bunches somewhat. This should be examined by a detailed tracking program.

The synchrotron, itself, may be troubled by this same limitation. A suggestion would be that the γ_t should be above the final energy to avoid accelerating the beam through transition. As n approaches zero, ρ

approaches unity but it might be acceptable in the synchrotron because this condition only exists for a relatively short time.

The author wishes to acknowledge valuable discussions with Lloyd Smith.

A SELF-CONSISTENT LONGITUDINAL DISTRIBUTION

by

L. Smith

This note is supplemental to the one by M. Barton, these proceedings, showing the existence of a self-consistent distribution function with space charge forces included which is also consistent with Barton's analysis. A similar distribution for linear forces has been given by Neuffer*; in this note, his work is recast into a form more suitable for the present purpose and does not invoke a linear approximation to the forces. The latter feature might be useful if space charge forces are significant for bunches which occupy a fair fraction of the RF bucket. The procedure used is to make use of the fact that any function of the constants of motion is a solution of Vlasov's equation, in particular, any function of the time-independent Hamiltonian.

The Hamiltonian for longitudinal motion is

$$H(u, \phi) = \frac{1}{2} \frac{h\eta}{\beta^2} u^2 + \frac{eV}{2\pi E} (1 - \cos \phi) + \frac{ZiZ}{nZ_0} \frac{r_p}{R} \frac{mc^2}{E} \beta h^2 (\lambda - \lambda_0) \quad , \quad (1)$$

where the canonical momentum if $u = \Delta E/E$, $\lambda(\phi) =$ number of particles per rf radian, $\lambda_0 = \lambda(0)$, r_p = proton classical radius, and

$$\frac{iZ}{Z_0 n} = \frac{g}{2\beta\gamma^2} = \frac{1 + 2 \ln(b/a)}{2\beta\gamma^2}$$

for a smooth conducting wall (Z_0 is the impedance of free space = 377 Ω). This Hamiltonian is also valid for a more general Z , provided that $i(Z/n)$ is independent of n and real. Consider the distribution function,

*D. Neuffer, Trans. IEEE NS-26, June 1979, p. 3031.

$$f(u, \phi) = \frac{2D}{\pi} \left[u_0^2 - v(1 - \cos \phi) - z(\lambda - \lambda_0) - u^2 \right]^{1/2} , \quad (2)$$

$$\text{with } v = 2 eV\beta^2 / 2\pi E h n, \text{ and } z = \frac{2iz}{nZ_0} \frac{r_p}{R} \frac{mc^2}{E} \beta h^2 \cdot \frac{2\beta^2}{h n} , \quad (3)$$

and D , u_0^2 , and λ_0 are to be determined. The function f is defined such that $\lambda(\phi) = \int f du$, with the normalization such that $\int f du d\phi = N$, the total number of particles in a bunch.

Then

$$\lambda = \int f du = D \left[u_0^2 - v(1 - \cos \phi) - z(\lambda - \lambda_0) \right] ,$$

whence $\lambda(0) = \lambda_0 = D u_0^2$, so that one can write

$$\lambda = \lambda_0 \left[1 - \frac{v}{u_0^2} (1 - \cos \phi) - \frac{z}{u_0^2} (\lambda - \lambda_0) \right] , \quad (4)$$

from which

$$\lambda - \lambda_0 = \frac{-\lambda_0 v (1 - \cos \phi)}{u_0^2 + z \lambda_0} ,$$

and thus,

$$\lambda = \lambda_0 \left[1 - \frac{v}{u_0^2 + z \lambda_0} (1 - \cos \phi) \right] . \quad (5)$$

At the limits of the bunch, $\pm\phi_m$, the density $\lambda = 0$, thus

$$\frac{v}{u_0^2 + z\lambda_0} (1 - \cos \phi_m) = 1 \quad , \quad (6)$$

and

$$\lambda = \frac{\lambda_0 v}{u_0^2 + z\lambda_0} [\cos \phi - \cos \phi_m] \quad . \quad (7)$$

Integrating this expression from $-\phi_m$ to ϕ_m gives the total number of particles in a bunch:

$$\begin{aligned} N &= \int_{-\phi_m}^{\phi_m} \lambda d\phi = \frac{2\lambda_0 \phi_m v}{u_0^2 + z\lambda_0} \left[\frac{\sin \phi_m}{\phi_m} - \cos \phi_m \right] \quad , \\ &= \frac{2\lambda_0 (\sin \phi_m - \phi_m \cos \phi_m)}{1 - \cos \phi_m} \quad (\text{from Eq. 6}) \quad . \end{aligned} \quad (8)$$

Thus in terms of the total number of particles in a bunch and the maximum phase extent of the bunch, the linear density at $\phi = 0$ is

$$\lambda_0 = \frac{N}{2} \frac{1 - \cos \phi_m}{\sin \phi_m - \phi_m \cos \phi_m} \quad , \quad (9)$$

and the fractional energy spread at $\phi = 0$ is given by, from Eqs. (6) and (9),

$$u_0^2 = (1 - \cos \phi_m) \left[v - \frac{(N/2) z}{\sin \phi_m - \phi_m \cos \phi_m} \right] . \quad (10)$$

Returning now to the distribution function given by Eq. (2), using Eqs. (5), (6), and (10) gives

$$f = \frac{2\lambda_0}{\pi u_0^2} \left[u_0^2 \frac{\cos \phi - \cos \phi_m}{1 - \cos \phi_m} - u^2 \right]^{1/2} , \quad (11)$$

so that the area of the bunch in volt-seconds is

$$\begin{aligned} A &= \frac{4E}{\hbar w} \int_0^{\phi_m} d\phi |u_{\max}(\phi)| , \\ &= \frac{4u_0 E}{\hbar w (1 - \cos \phi_m)^{1/2}} \int_0^{\phi_m} d\phi [\cos \phi - \cos \phi_m]^{1/2} , \\ &= v \left[- \frac{(N/2) z}{\sin \phi_m - \phi_m \cos \phi_m} \right]^{1/2} \frac{E}{\hbar w} I(\phi_m) , \end{aligned} \quad (12)$$

where

$$I(\phi_m) \equiv 4 \int_0^{\phi_m} d\phi [\cos \phi - \cos \phi_m]^{1/2} = 8\sqrt{2} \left[E\left(\sin \frac{\phi_m}{2}\right) - \cos \frac{\phi_m}{2} F\left(\sin \frac{\phi_m}{2}\right) \right] \quad (13)$$

where F , E are elliptical integrals of first and second kind, respectively.

Then

$$v = \frac{(N/2) z}{\sin \phi_m - \phi_m \cos \phi_m} + \left(\frac{h w A}{EI} \right)^2 , \quad (14)$$

so that, finally, the voltage required to confine a bunch of emittance A to a phase range $\pm \phi_m$ is, by Eqs. (14) and (3)

$$\frac{h e V}{2\pi} = \frac{h^4 w^2 n}{2\beta^2 E} \frac{A^2}{I^2} + \frac{iZ}{nZ_0} N \frac{r_p}{R} \frac{mc^2}{\beta} \frac{h^3}{[\sin \phi_m - \phi_m \cos \phi_m]} \quad (15)$$

For $\phi_m \ll 1$, Eq. (15) is identical with the one used by Barton, remembering that rf phase is used in this note, larger than his by a factor, h . It is interesting to note that if iZ/n is negative, as it might well be, the required voltage is reduced in the presence of space charge. However, in that case the beam is subject to a micro-wave instability and the threshold for that effect must be examined.

RAPID-CYCLING TUNED rf CAVITY FOR SYNCHROTRON USE

by

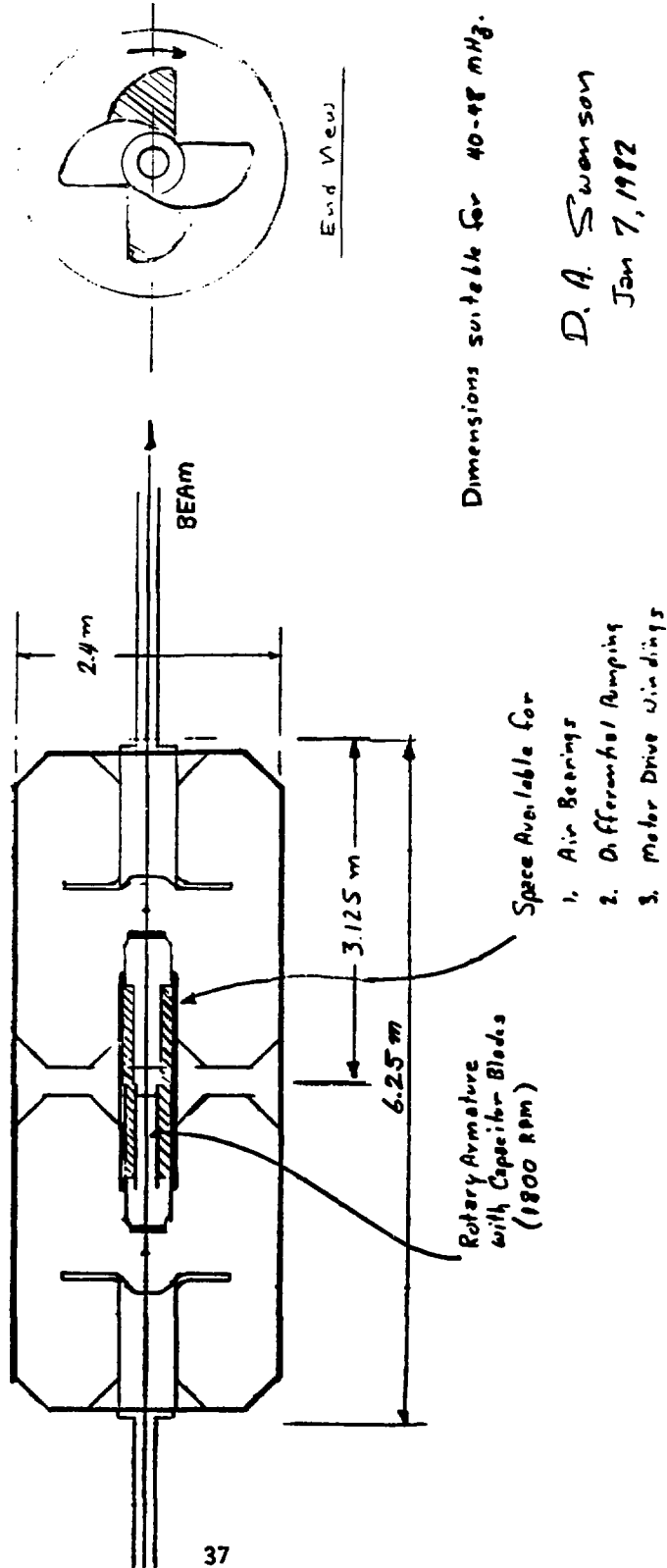
D. A. Swenson and J. M. Potter

Ferrite-tuned rf cavities for synchrotron use tend to be low in efficiency, especially when a large frequency swing is required. A mechanically-tuned cavity is suggested in this note which has a very much higher efficiency, and which should be suitable for rapid-cycling synchrotron use with any required frequency swing.

The tuning is accomplished by rotation of a few-bladed propeller on one side of the acceleration gap against a stationary propeller blade on the other side of the acceleration gap. In the configuration suggested here, both propeller blades are mounted on hollow tubes through which the beam passes. This results in a variable capacitor in the center of the cavity where the electric fields are high and the magnetic fields are low. This is the optimum location for a variable capacitor which must have a large effect on the resonant frequency of the cavity without introducing large power losses to degrade the efficiency of the structure.

Frequency range	40 to 48 MHz
Repetition rate	60 Hz
Peak voltage	10 MV
Number of cavities	4
Shunt impedance/cavity ZT_L^2 =	25 M Ω
Power/cavity $P_c = \Delta V^2/ZT_L^2 =$	250 kW
Power (total) $P_t = 4 \cdot P_c =$	1 MW

RAPID-CYCLING TUNED CAVITY FOR SYNCHROTRON USE



CONSIDERATIONS ON A HIGH SHUNT IMPEDANCE TUNABLE rf CAVITY

by

P. L. Morton

In this note I will run through some quick calculations relating to the cavity proposed by Swenson and Potter (see previous paper).

The first consideration concerns the varying energy stored in the cavity as the frequency changes from 40 to 48 MHz. The time of this swing is about 8 ms up followed by 8 ms down. Thus

$$\frac{\Delta\omega_{rf}}{\Delta t} = 2\pi \times 10^9 \text{ rad/s} .$$

Noting that $\Delta\omega_{rf} \ll \omega_{rf}$ in $\Delta t = 2\pi/\omega$ allows us to observe that ωW is an adiabatic invariant, whence

$$W = \left(\frac{\omega_{rf}}{\omega_0 \text{ rf}} \right) W_0 ,$$

and

$$\frac{dW}{dt} = \frac{W_0}{W_0} \frac{d\omega_{rf}}{dt} .$$

Taking $W_0 = 52 \text{ J}$, $W_f = 62 \text{ J}$, $\omega_0 \text{ rf}/2\pi = 4 \times 10^7 \text{ rad/s}$, and $dW/dt = 1300 \text{ W}$ ($= 1.75 \text{ HP}$), we could use a flywheel to supply energy to the cavity. As ω

increases, the flywheel loses 10 J and as ω decreases, the flywheel gains 10 J. The power delivered to the cavity is

$$P = L\omega_{FW} = L \frac{2\pi}{16 \times 10^{-3}} ,$$

which implies, since $P = 1300$ W, that the torque L is 3.31 N m, a modest torque. We want the stored energy in the flywheel to be much greater than 10 J, that is,

$$\frac{1}{2} I\omega^2 \gg 10 \text{ J} .$$

For $\omega = 2\pi/16 \times 10^{-3} = 392$ rad/s, this gives $I \gg 1.3 \times 10^{-4}$ kg m², which is a pretty small flywheel. The flywheel could easily consist of the rotating blades themselves, which must be designed taking into account the fact that as energy enters the cavity the flywheel slows down.

Secondly, let us consider matching of the beam-loaded cavity to the generator so as to minimize the reflected power. For a 3 MV cavity with a shunt resistance of 27 M Ω , the generator current in the absence of beam loading would be $I_{go} = V_0/R_0 = 3/27 = 0.111$ A, with the phase relationship between voltage and current as indicated in Fig. 1.

For a synchrotron accelerating from 800 MeV to 4 GeV in 8 ms and a revolution period of 3×10^{-6} s (140 m average radius), the acceleration takes place in 2700 turns. The stable phase angle will be approximately given by

$$\sin \phi_s = \frac{1}{eV} \frac{dE}{dn} = \frac{3200 \text{ MeV}}{2700 \text{ turns}} \frac{1}{3 \text{ MeV}} \approx 0.40 .$$

Thus $\phi_s = 24^\circ$ and $\cos \phi_s \approx 0.92$. As the beam current I_b increases we will need to increase I_g (the generator drive) and to detune the resonance frequency of the cavity relative to the drive frequency of the generator.

Referring to the phasor diagram, Fig. 2, we have the following relations: The admittance $Y = 1/R(1 + j \tan \phi_Y)$. [Note that ϕ_Y has a negative value in the diagram.]

$$YV = -(I_g + I_b) .$$

Taking the real part of this last relation gives

$$I_g = 0.111 + I_b \sin \phi_s \quad 0.111 + 0.4 I_b \text{ A} , \quad (1)$$

for constant voltage and no reflected power. Taking the imaginary part gives

$$\tan \phi_Y = \frac{-RI_b \cos \phi_s}{V} , \quad (2)$$

again for no reflected power and constant voltage. The effective admittance seen by the generator is

$$Y_{\text{eff}} = -\frac{I_g}{V} = \frac{1}{R_{\text{loaded}}} , \quad (3)$$

For $I_b = 1 \text{ A}$, $I_g = 0.51 \text{ A}$, and $R_{\text{loaded}} = 5.88 \text{ M}\Omega$. Evaluating ϕ_Y from Eq. (3) gives $\phi_Y = -83.1^\circ$.

Finally, let us consider the Robinson instability, which requires us to detune the cavity such that

$$\frac{-2V}{I_b R} \cos \phi_s < \sin 2\phi_Y < 0 .$$

Define $I_{bc} = 2V \cos \phi_s / R = 0.204 \text{ A}$. For beam currents greater than I_{bc} , ϕ_Y will be restricted to lie outside a region about -45° , as sketched qualitatively in Fig. 3. For $I_b < I_{bc}$ both the Robinson stability

criterion and the condition for no reflected power can be simultaneously satisfied. For $I_b > I_{bc}$ we want

$$\tan \phi_y = -\frac{RI_b}{V} \cos \phi_s \quad (\text{constant } V, \text{ no reflected power}) ,$$

or

$$\phi_y = \phi_{y1} = -\tan^{-1} \frac{-RI_b \cos \phi_s}{V} .$$

For Robinson stability we want

$$\phi_y > \phi_{y2} = -\left[\frac{\pi}{2} - \frac{1}{2} \sin^{-1} \left(\frac{2V}{RI_b} \cos \phi_s \right) \right] .$$

Let $x = RI_b/V$. Table I shows ϕ_{y1} and ϕ_{y2} as a function of x .

TABLE I

<u>I_b (amps)</u>	<u>x</u>	<u>$-\phi_{\gamma 1}$</u>	<u>$-\phi_{\gamma 2}$</u>
0.204	1.84	59.4°	45.0°
0.222	2.0	61.5°	57.2°
0.333	3.0	70.1°	71.3°
0.444	4.0	74.8°	76.5°
0.555	5.0	77.7°	79.3°
0.666	6.0	79.7°	81.2°
0.777	7.0	81.2°	82.5°
0.888	8.0	82.3°	83.4°
0.999	9.0	83.1°	84.2°

Note that for $I_b > 0.3$ A we need to detune the cavity a few extra degrees (more than for zero reflected power) in order to satisfy the Robinson instability criterion.

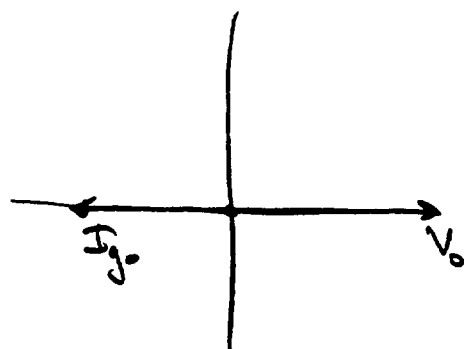


Fig. 1

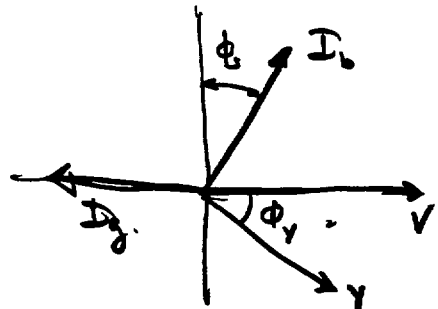


Fig. 2

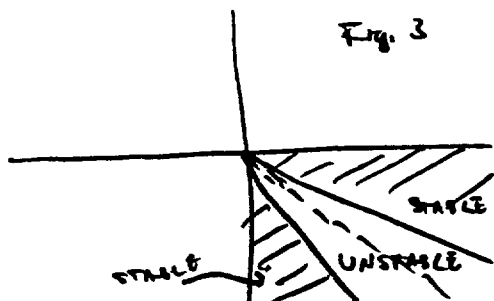


Fig. 3

ROTATING CONDENSERS

by

M. Foss

Because there is current interest in this type of equipment I, would like to tell you about the Carnegie Institute of Technology rotating condenser. Our condenser has had over ten years of satisfactory operation.

One interesting feature is the main bearings. These are 120° nylon sleeve bearings operating in cooled Myvane oil. The 240° anulus not occupied by the bearing is used as an oil duct. The original nylon sleeves are still in service and show no perceptible wear.

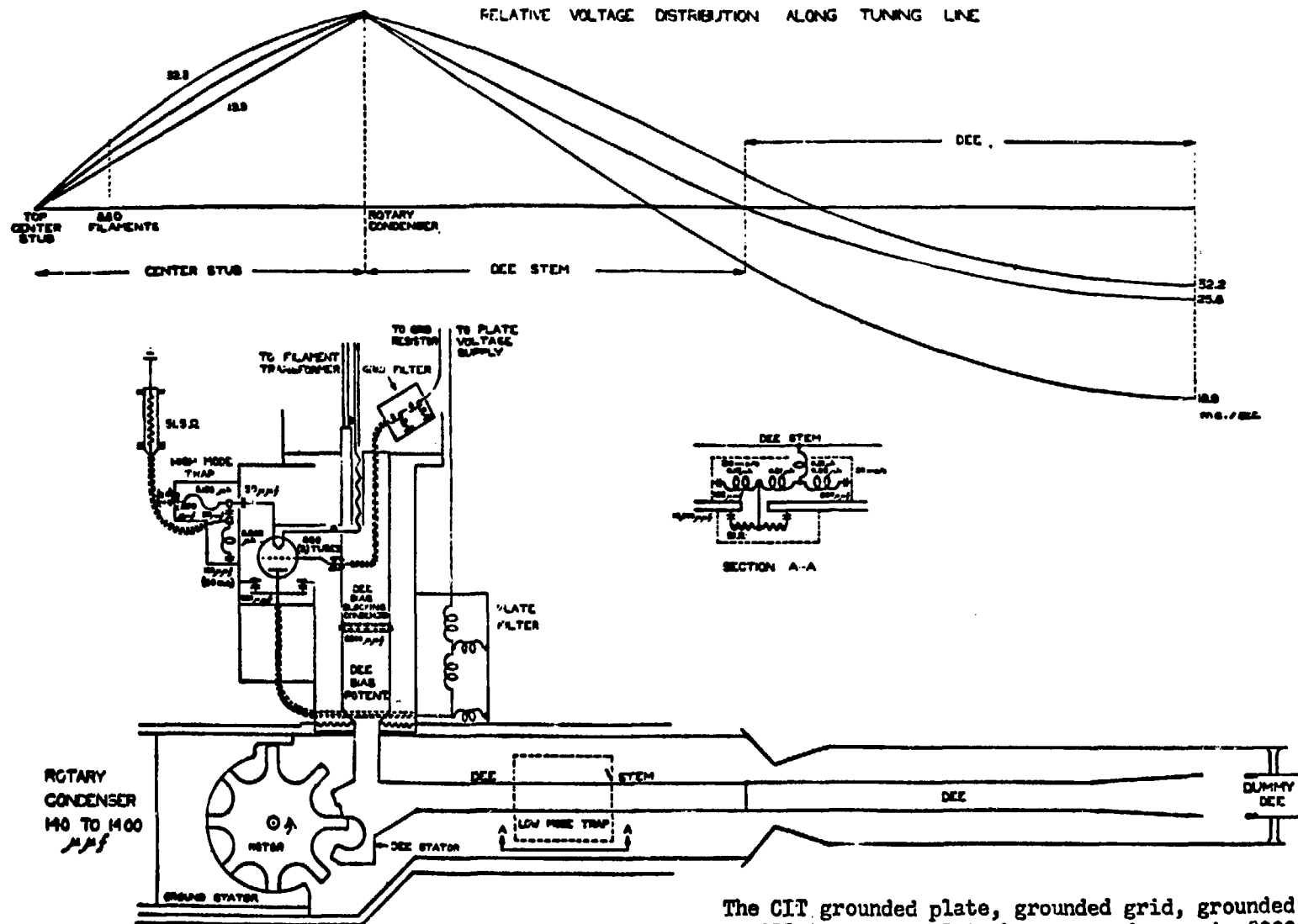
The main bearing oil is kept out of the vacuum by modified 3-1/2 in. Crane seals. The rotating seal is made between a ceramic alumina ring and a non-porous graphite ring. The original seal between the shaft and the rotating ring has been replaced by an "O" ring. The spring which holds the rings together has its turns shorted together with braid to prevent rf resonances.

If the condenser shaft has an axial resonance in the band of frequencies required for acceleration, the oscillator may not operate at this frequency. To keep the axial velocity high (in a line which is necessarily capacity loaded) the inductance was kept at a minimum. The axial velocity in the 1-m-long toothed region is $c/3$. By using an appropriate impedance between the toothed region and the bearings a resonant frequency of 33 megacycles/s was achieved.

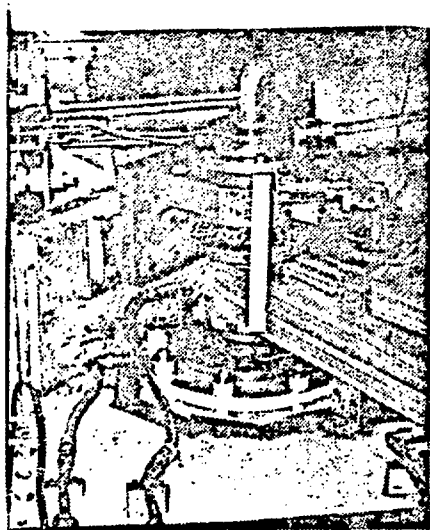
One end of the shaft sticks out of the vacuum tank. It is used for a drive sheave, thrust bearing, and shaft water cooling connections. This end was subject to excessively high rf voltages which broke the bearing bracket insulators. To overcome this problem the bearing bracket was grounded and the shaft connected to the bearing bracket by brushes. There are now two resonances, one at 5 and one at 40 megacycles/s.

Our condenser was designed to deliver 400 pulses/s (3000 RPM) and use 50% of the time accelerating beam. However, we operate at 200 pulses/s.

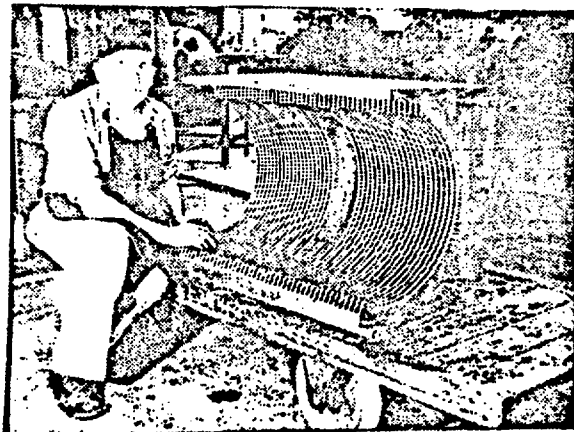
The brushes and water seal limit the speed. Both of these will be improved to allow operation at 300 pulses/s. It is not clear that we will be able to reach 400.



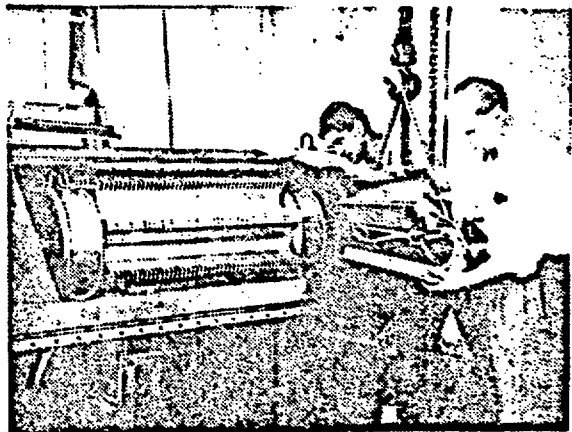
The CIT grounded plate, grounded grid, grounded cathode oscillator. The plate bypass condenser is $8000 \mu\mu f$ (note error), grid bypass $1200 \mu\mu f$ each, and filament bypass $70,000 \mu\mu f$. The outstanding drawback to this system is the low impedance which the tubes drive.



Bearing insulation and oil pipes, the optical commutator, belts, brushes, bearing bracket, and water seals. This region acted as a step up transformer when the bracket was insulated from ground. To avoid this the bracket was grounded and brushes were installed to ground the shaft.



Ground Stator - The hole was put in for pumping. 5 rows of rotor teeth are in the stator at maximum capacity.



Condenser Assembly - Note that the teeth are cut only deep enough to give the required clearance, 2 mm. in the ground stator and 3 1/3 mm. in the "D" stator. This minimizes the axial inductance.

SLOW EXTRACTION FROM THE STRETCHER RING

by

J. STAPLES

An outline for a third-integer slow extraction system for the 16-GeV stretcher ring is presented. No major obstacles are seen in extracting a beam with an average thermal power of 1.5 MW. Short rf microstructure may be possible.

The relevant parameters of the stretcher ring are listed below:

\bar{R}	142 m
Stored particles	10^{13} p/cycle
Flux	6×10^{14} p/s
radial emittance	$1.7 \pi \text{ mm-mmrad}$
T	16 GeV
cycle time	16.7 ms

There is no problem in storing 10^{13} 16-GeV protons in a ring of this size. However, no extraction system has operated with an average beam flux of 6×10^{14} p/s. Therefore, attention is paid to the thermal consideration for the first septum.

In order to reduce both beam interception by the septum and the extracted beam emittance, a 0.006 cm (2.5 mil) foil electrostatic septum, followed by a thin (0.5-cm) one-turn magnetic septum, is used. The required beam growth per 3 turns for a 99% extraction efficiency is 0.6 cm/3 turns. A 5-part electrostatic septum is used, constructed of 5 units, each 1 m long, operating at a gradient of 10 MV/m. With all 5 units operating, the extracted beam at the end of the septum is displaced 0.74 cm from the circulating beam envelope.

The septum material will be titanium and will dissipate 6.5 W/cm as it intercepts a flux of 6×10^{12} /sec of 16 GeV protons. A foil 0.8 cm high will attain a peak temperature of 1000°C if only conduction is considered. It would probably be destroyed if it intercepted the full circulating beam.

One or more of the electrostatic units may be disabled and removed from the beam if it is damaged while still permitting adequate displacement for the magnetic septum.

We will follow the electrostatic septum with a 0.5 cm thick edge-cooled single-turn magnetic septum with a 1 cm vertical gap 2 m long. The current density of $10\ 000\ A/cm^2$ dissipates 35 kW in the conductor. At the end of the magnetic septum, the extracted beam is displaced 6.8 cm from the edge of the circulating beam.

A third integer extraction will contain the initial beam inside a separatrix area of $5\pi\ mm\cdot mrad$. The septum location will be 2-3 times further out than the nearest fixed point or about 3 cm off the central orbit, implying at least a 6 cm radial aperture around the machine. The extracted beam emittance with a 6 mm/3 turn jump will be less than $1\pi\ mm\cdot mrad$, unnormalized.

The entire beam must be extracted in less than 5600 turns. Fast resonant extraction has been demonstrated at both FNAL and BNL.

A short rf microstructure of 0.5 ns or less is desirable for TOF separation of secondary π and K beams. The beam will be bunched at the $994 = 142 \times 7$ harmonic, or 334 MHz. Without additional considerations, the extracted bunch length would be 1 ns. However, if the position of the stable area is made energy dependent by introducing a non-zero chromaticity, particles whose energies are at the top of the bucket may be extracted preferentially, sharpening the microstructure by approximately a factor of 2. The computer codes necessary to study this effect in detail have not yet been written.

AN ANTIPROTON SOURCE FOR LAMPF-II

by

J. Simpson

The large average current ($\sim 100 \mu\text{A}$) of protons anticipated from LAMPF-II tempts one to see if it can be used to produce a useful, competitive \bar{p} source. Uses might include \bar{p} beams for low energy (a few hundred MeV) fixed target physics and for higher energy ($\sim 10 \text{ GeV}$) \bar{p} -p collider physics. The physics justifications will be somewhat subjective, but I suspect that the existence of CERN's antiproton projects and of FNAL's soon-to-be-built one will probably mean that unless a new source has some very unique properties, the interesting experiments will have long been done before LAMPF-II operates.

I have estimated what the performance of a LAMPF-II \bar{p} source might be based on known cooling techniques and extrapolated information.

p PRODUCTION

Comparative measurements at CERN suggest that the \bar{p} yield (forward and small $\delta p/p$) from 18 GeV protons is about half that at 24 GeV. The \bar{p} production target for the CERN AA yields $\sim 2.5 \times 10^{-6} \bar{p}/\text{p}$ into a $100\pi \times 100\pi \times 1.5\% \delta p/p [\text{mm} \cdot \text{mrad}]^2$ acceptance. Since the "natural" slug of protons available from LAMPF-II will be $\sim 10^{13}$, we might expect $\sim 10^7 \bar{p}/\text{cycle}$ at $\sim 2.5 \text{ GeV}$ into a similar acceptance. I'm also told that perhaps 1/6 of the synchrotron output may be available for \bar{p} s, so we may have an average flux of $10^8 \bar{p}/\text{s}$. The problem is how to use them. It isn't realistic to consider deceleration for such large emittances down to a few hundred MeV for fixed target work. Thus some sort of cooling must be implemented.

COOLING CONSIDERATIONS

Electron cooling times are strong functions of γ , as much as γ^4 . Even at 200 MeV, cooling times are 1/2 to 1 s, so that at 2.5 GeV the rate is

prohibitively slow. Similarly, characteristic cooling times for stochastic cooling of 10^7 particles are also ~ 1 s. A "brute force" straightforward cooling step before deceleration doesn't appear to be acceptable.

A PLAUSIBLE COOLING SCHEME

Consider the following scenario. Bear in mind that some numbers are "soft".

- Accelerate 10^{13} p to 16 GeV and attain a bunch width of about 2 ns (less if possible). Single turn extract and target.
- Accept, at 2.5 GeV, \bar{p} 's into perhaps $50\pi \times 50\pi \times 2\% \frac{\delta p/p}{(\text{mm-mrad})^2}$. Scaling from CERN's AA, we might expect

$$2.5 \times 10^7 \times \sqrt{\frac{(\epsilon_x \epsilon_y)_L}{(\epsilon_x \epsilon_y)_C}} \frac{(\delta p/p)_L}{(\delta p/p)_C} \approx 8 \times 10^6 \bar{p}'s$$

- Debunch the \bar{p} 's (they still have the synchrotron bunch structure, 2 ns spaced 20 ns) by one of two ways:
 - Linear debunching (Either drift the beam or, better, pass it through a time dispersive transport to shear the bunches in time. The $\pm 1\% \delta p/p$ corresponds to ± 25 MeV, so 50-100 MeV of h.f. cavity can effectively debunch by a factor of 5 or so).
- or
- Inject the beam into a circular debuncher ring in which the bunches are contained in large but mismatched rf buckets. After roughly 1/4 to 3/8 of a turn in the bucket, remove the rf. This is the scheme proposed in the FNAL \bar{p} source.

At this point then, the \bar{p} 's would have an energy spread of 5 to 10 MeV (f.w.)

- Inject the "debunched" beam into a cooling ring where the following sequence occurs.
 - The injected beam is rf stacked to the bottom of a stochastic stacking system. This process can further reduce the momentum spread, if necessary, to 5 MeV (f.w.).

- A stochastic stacking system stacks the beam into an exponentially increasing (with energy) density distribution. The density, $\psi \equiv \# \text{ particles/eV}$, will vary by two or more orders of magnitude over a stack width of 20 MeV or so. The stacking time, defined by the approximate time it takes an injected particle to reach the stack top, will be about two minutes.
- Simultaneously, a transverse cooling system will be cooling betatron emittances. This might be separate x,y-cooling or just y-cooling with x-y coupling in the orbit dynamics. It will result in an emittance reduction of a factor of ~ 10 in each plane. I've estimated this from the FNAL design and from CERN's performance in which similar factors are obtained with effective cooling times of 1800 s. This is 15 times longer than the 2 minute stack, but the effective number of particles in the betatron cooling channel is at least two orders of magnitude larger in the CERN case than in the LAMPF-II stack.
- Periodically rf unstack a small bunch from the stack top, transfer it to a decelerating ring (maybe the 4 GeV booster on its way down), decelerate the beam to the desired energy, extract and target.

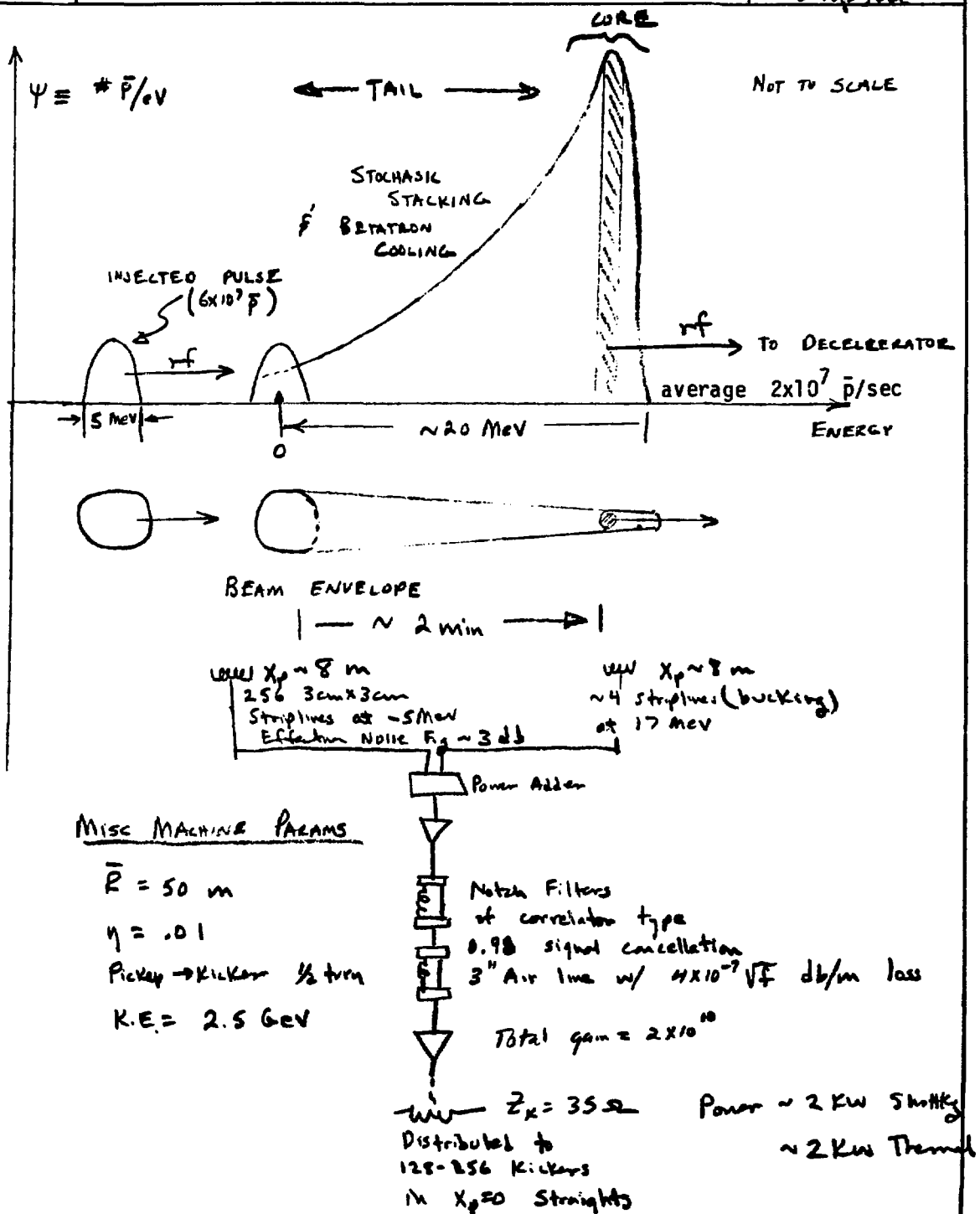
This sequence is depicted in Fig. 1, along with a first attempt to model the hardware.

Preliminary computer simulations indicate that with some optimization of this first pass system, the beam may be delivered to the stack tail at a 3 Hz rate and still be efficiently brought into the stack. Thus the total \bar{p} flux available at the stack top will be, at most, about $3 \times 8 \times 10^6 = 2.4 \times 10^7 \text{ p/s}$. This is midway between CERN's AA (10^7 p/s) and FNAL's TEV-I ($4-5 \times 10^7 \text{ p/s}$). This stacking scheme can be modified to produce much higher stack peak density and a wider stack. Such a stack would be needed if the high density core were to be extracted to a collider.

CONCLUDING COMMENTS

It is interesting that this system, CERN's, and FNAL's are very close in design \bar{p} flux. This closeness reflects the state of the art in stochastic cooling. How can one do better? More parallel systems (Russ Huson approach)

would be a brute force solution. Otherwise, even if the target would survive more incident protons/pulse, the increased \bar{p} yield would slow down the cooling to diminish the potential gain. Some gain (<2) might be obtained by increasing the stochastic system bandwidth to 2-4 GHz. I should comment that the cost of this source won't be cheap. The total stochastic cooling power installed must be at least twice that produced by thermal and Schottky noise. At \$800/W for 1-2 GHz broadband amps, the amplifiers alone will be \$5 million or better. The total stochastic cooling system will run at least another \$1 million. I'm not going to attempt a careful cost estimate, but the total \bar{p} source (transports, targets, debuncher, accumulator, etc.) will probably cost \$20 to 30 million. Competition from by then existing \bar{p} sources will be tough to beat since a few $\times 10^7$ \bar{p} rates will already exist and a few GeV X few GeV collider is relatively inexpensive. The FNAL 8 GeV debuncher could even be used with some modification.



STACKING DISTRIBUTIONS + SYSTEM

Fig. 1

5

KINETIC ENERGY

2.500E+00

GAMMA

3.665E+00

BETA

9.621E-01

ROTATION FREQ.

9.187E+05

ETA

1.000E-02

KAPPA

1.814E-05

DE INJECTED

5.000E+06

DE OF STACK

4.000E+07

DF/FO (1)

8.737E-01

ENTER 2 FOR INJECTION

3 FOR POWER

4 FOR GPlOTS

5 FOR READ

6 FOR WRITE

7 TO READ NAMELIST

8 TO PRINT NAMELIST

9 TO TERMINATE RUN

? 8

1BX

QUL

• 1E+10, .1E+10, .2E+10, .1E+10, .2E+09,

QUN

• .2E+10, .2E+10, .4E+10, .2E+10, .12E+10,

QNSVS

• 1,

QNPAR

• .5E+07,

QTE

• .25E+10,

QDEx

• .4E+08,

QDEINJ

• .5E+07,

QMPU

• 256, 128, 64, 64, 1,

QWKICK

• 256, 256, 256, 64, 1,

QTBDELAY

• 0.0, 0.0, 0.0, 0.0, 0.0,

QTBAD

• .5E+02,

QETA

• .1E-01,

QMPK

• .2E+01, .2E+01, .2E+01, .2E+01, .2E+01,

QXPP

• .2E+01, .2E+01, .2E+01, .2E+01, .2E+01,

QSEP

• .5E+00, .5E+00, .4E+00, 0.0, 0.0,

QG1

• .2E+11,

QG2

• .1E+07,

QG3

• .3E+01,

QG4

• .99E+00,

QG5

• .5E+01,

QME

• 101,

QCPUTL

• .63E+02,

QEND

ENTER 2 FOR INJECTION

3 FOR POWER

4 FOR GPlOTS

5 FOR READ

6 FOR WRITE

7 TO READ NAMELIST

8 TO PRINT NAMELIST

9 TO TERMINATE RUN

? 3

THEMM PWR INTO 35.0MH LOADS(1)

5.665E+03

USE EXISTING PSI OR INJECTED ONLY(1 OR 2)?

? 1

SHOTT. PWR INTO KICKER(1)(35.0MH)=

8.73E+08

ENTER 2 FOR INJECTION

3 FOR POWER

4 FOR GPlOTS

5 FOR READ

6 FOR WRITE

7 TO READ NAMELIST

8 TO PRINT NAMELIST

9 TO TERMINATE RUN

? 3

THEMM PWR INTO 35.0MH LOADS(1) 5.665E+03

USE EXISTING PSI OR INJECTED ONLY(1 OR 2)?

? 2

SHOTT. PWR INTO KICKER(1)(35.0MH)= 1.49E+03

ENTER 2 FOR INJECTION

3 FOR POWER

4 FOR GPlOTS

5 FOR READ

6 FOR WRITE

7 TO READ NAMELIST

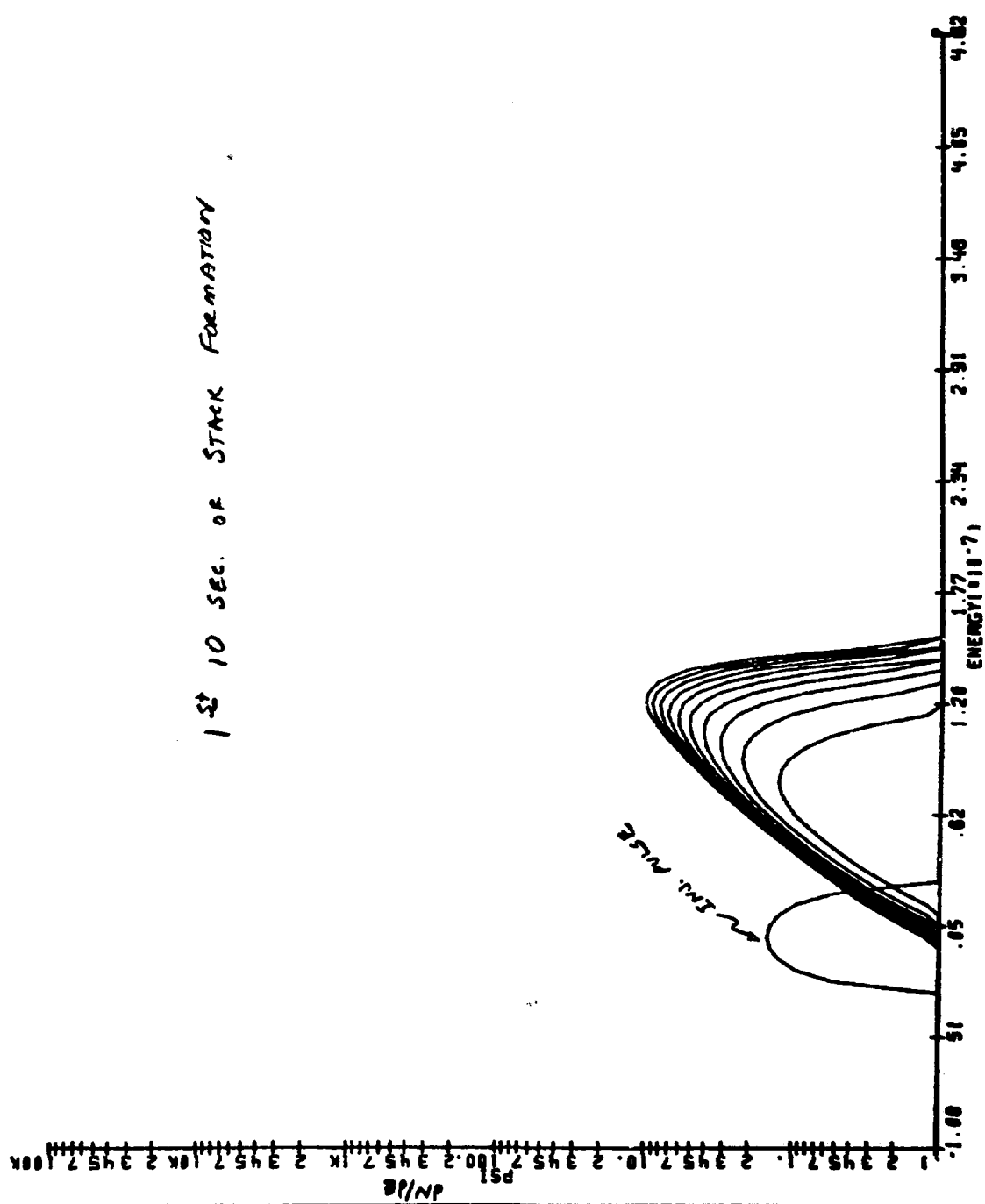
8 TO PRINT NAMELIST

9 TO TERMINATE RUN

?

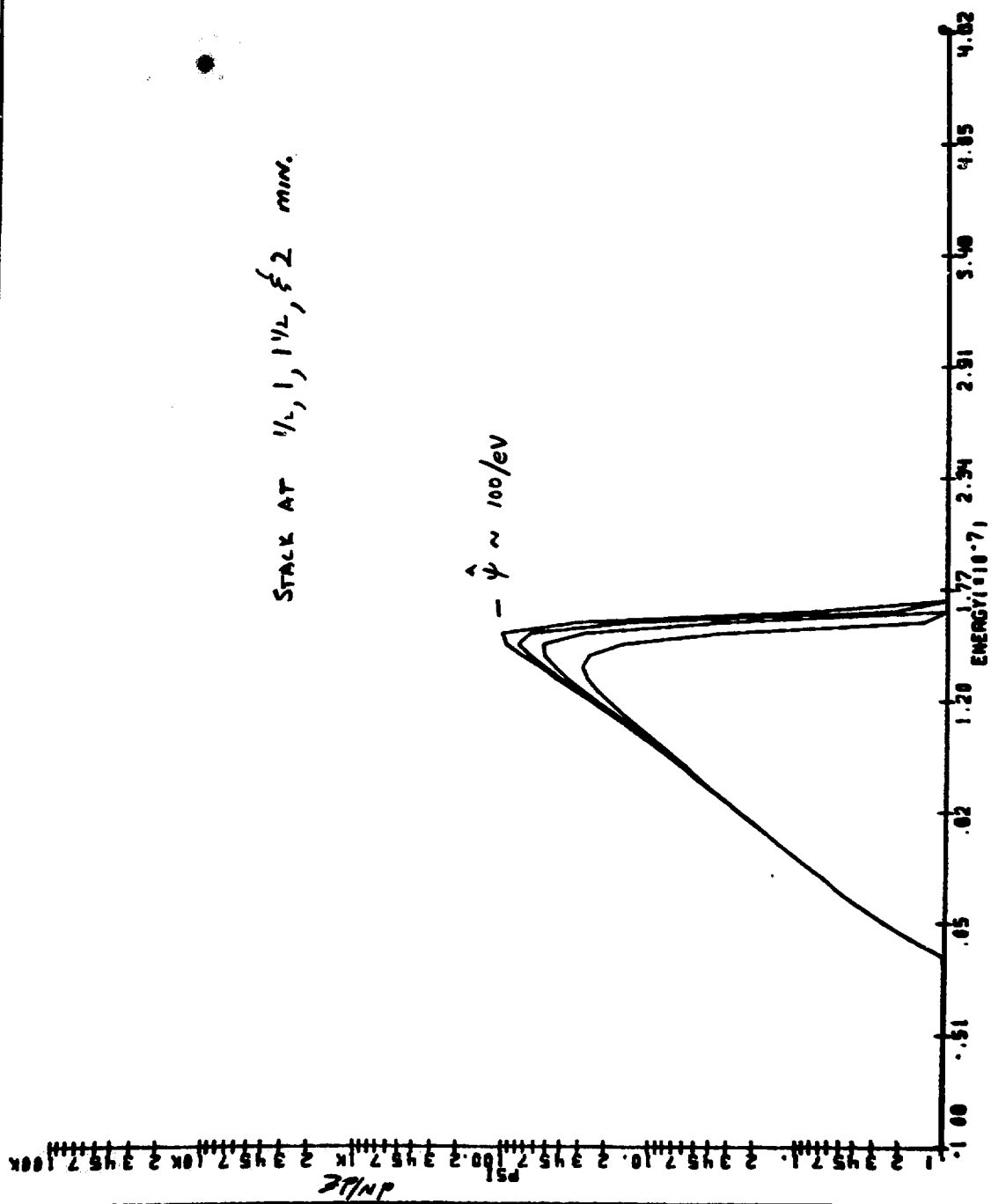
- can surely be reduced

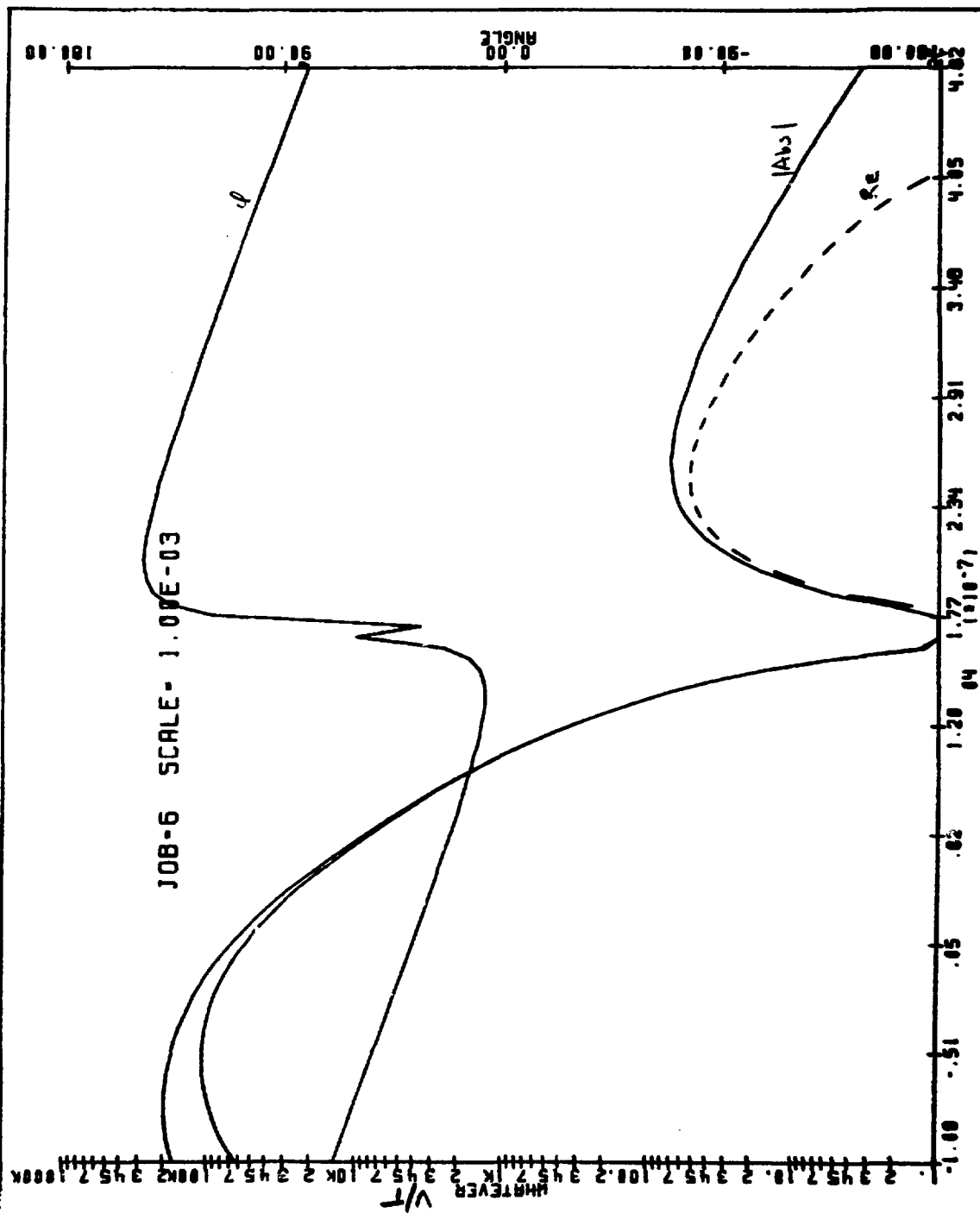
1st 10 sec. of stack formation



Stack At $1/2, 1, 1 \frac{1}{2}, \frac{3}{2}$ min.

$$-\hat{\psi} \sim 100/\text{eV}$$





V/turn produced by Modulated System

SYNCHROTRON MAGNET CIRCUIT

by

M. Foss

A useful form for the current in a rapid cycling synchrotron is a sine wave added to a dc bias. In the White circuit the dc is delivered through a choke and the ac through a condenser. The choke carries the ac in the "wrong" direction. The ideal choke would have minimum dc resistance and maximum inductance and could be very costly. If the cost of the synchrotron system is minimized then the cost of the choke is a fair fraction of the cost of the synchrotron magnet.

With a rapid cycling booster feeding a rapid cycling synchrotron it is possible to use one machine as a choke for the other. There are two matching conditions: both machines must use the same dc current and both machines must use the same ac voltage. In our case this means that the booster energy must be greater than 4 GeV or the booster gap volume must be oversized or both. Alternatively an inductance could be put in series with the booster to make the circuits match. Some flexibility in shaping the ac wave forms is lost, and staging is more difficult.

The ac synchrotron flux can be returned in a second gap adjacent to the synchrotron gap. The dc bias field is supplied by a coil around both gaps which therefore links no ac flux. This will simplify regulation of the bias current. The dc field could be supplied by a stable superconducting coil if this were desirable.

The return flux gap need not be identical to the synchrotron gap. With an optimized return flux gap the magnet system may cost less than the separate magnet and choke employed in the White circuit. The figures below present simplified geometries, easy to calculate. The cost factors are rough 1977 costs. The cost of the separate magnet and choke is \$1.64 million. The cost of the magnet-choke combination is \$1.49 million.

The magnet-choke combination lends itself well to a combined function machine. Quadrupoles which incorporate this principle can be designed.

***** 10/3/77 RUN #3 ***** PAGE 14
800,000,000 MeV HIGH INTENSITY PROTON SYNCHROTRON

S1: SYNCHROTRON & SEPARATE CHOKE

61: S1: WIDTH OF MAGNET COIL (M) = 0.141889168762
62: S1: LENGTH OF CHOKE YOKE = 0.77622853877
63: S1: WIDTH OF CHOKE COIL = 0.218196257894
64: S1: WIDTH OF CHOKE COIL GAP = 0.941832703964
65: S1: MAGNETIC FIELD IN CHOKE = 0.984654617917
66: S1: CHOKE TURNS / MAGNET TURNS = 0.409127480363

1: LIFE COST OF DC POWER (\$/W) = 0.6
2: LIFE COST OF AC POWER (\$/W) = 0.6
3: COST OF DC COPPER (\$/CUBIC M.) = 70000
4: COST OF AC COPPER (\$/CUBIC M.) = 100000
5: COST OF DC STEEL (\$/CUBIC M.) = 5900
6: COST OF AC STEEL (\$/CUBIC M.) = 28000
7: DC MAGNETIC FIELD IN GAP (T) = 0.454557553109
8: AC MAGNETIC FIELD IN GAP (T) = 0.242712446891
10: MAGNETIC FIELD IN AC STEEL (T) = 1.8
12: SPACE FACTOR IN AC COIL = 0.5
14: SPACE FACTOR IN AC STEEL = 0.95
15: COST OF CONDENSERS (\$/J) = 0.4
16: GAP HEIGHT (M.) = 0.2
17: GAP WIDTH (M.) = 0.35
18: LENGTH OF ONE BENDING MAGNET = 1.3744529494
19: NUMBER OF MAGNETS = 32
20: COST SADDLE/ COST RACETRACK = 1.2
21: MINIMUM MAGNETIC FIELD = 0.211845106219
22: MAXIMUM MAGNETIC FIELD = 0.69727
23: INJECTION ENERGY = 1.0E+8
24: FINAL ENERGY = 8.0E+8
25: BETA AT INPUT ENERGY = 0.42020776815
26: GAMMA AT INPUT ENERGY = 1.10658601953
27: BETA AT EXTRACTION ENERGY = 0.841821357162
28: GAMMA AT EXTRACTION ENERGY = 1.95268815628

***** 18/5/77 RUN #3 ***** PAGE 15
 800,000,000 NEW HIGH INTENSITY PROTON SYNCHROTRON
 S1 CONTINUED

ORBIT RADIUS = 7.09003139024 SACITA = 0.0337070644472
 SYNCH DC AMP TURN = 72245.0914971 SYNCH AC AMP TURN = 28628.8856726
 CHOKE DC AMP TURN = 29598.3609097 CHOKE AC AMP TURN = 29418.5328019
 CHOKE DC FIELD = 0.453705578111 CHOKE AC FIELD = 0.453949039866

S1: MAGNET COIL Cu = 240632.910134 \$ AC POWER = 76378.2272572 .
 DC POWER = 539239.8553094 .
 COIL GAP WIDTH = 0.35 COIL % GAP HEIGHT = 0.2
 CONDUCTOR WIDTH = 0.141089168762 JUMPER SEPARATION = 0.2

S1: MAGNET STEEL \$ STEEL = 173363.860785
 STEEL GAP WIDTH = 0.533778337524 STEEL LENGTH = 1.2744529494
 STEEL WIDTH = 0.83425118004 STEEL HEIGHT = 0.260286421258

TOTAL COST OF MAGNET (\$) = 1036112.65127

S1: CHOKE COIL \$ COPPER = 110631.19143
 DC POWER = 125558.00843 .
 COIL GAP WIDTH = 0.941832702964 COIL % GAP LENGTH = 0.03197914912
 CONDUCTOR WIDTH = 0.218196257894 COIL CAP LENGTH = 0.558634260876

S1: CHOKE STEEL \$ STEEL = 211298.639357
 STEEL GAP WIDTH = 1.37822521975 STEEL LENGTH = 0.7622053877
 STEEL WIDTH = 1.63845317766 STEEL HEIGHT = 0.1711035355

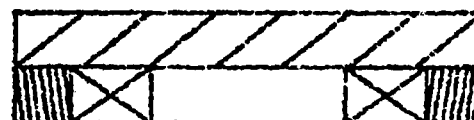
TOTAL COST CHOKE = 583698.31926

CHOKE AC ENERGY = 162357.954772 99831.7692869 $\epsilon = 250$ kVAr

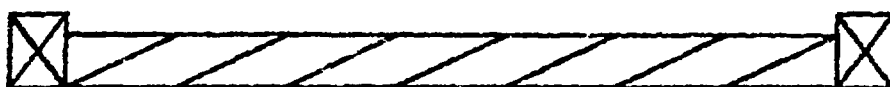
MAGNET AC ENERGY = 87221.4684457
 COST OF CONDENSERS =

S1 TOTAL COST 1639642.73982

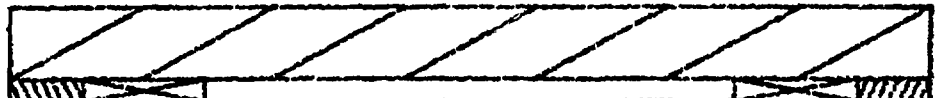
***** 10/5/77 RUN #3 ***** PAGE 13
900,000,000 MeV HIGH INTENSITY PROTON SYNCHROTRON
S1: CHOKES



S1 MAGNET CROSS SECTION (DASH=0.1 m.)



LENGTHWISE SECTION OF MAGNET



CROSS SECTION OF CHOKES



LENGTHWISE SECTION OF CHOKES

***** RUN #2 ***** PAGE 16
 800,000,000 10/6/77 HIGH INTENSITY PROTON SYNCHROTRON
 S21: COMBIHFD SYNCHROTRON AND CHOKE

51:	521:	522:	523:	524:	525:	526:	527:	528:	529:	530:	531:	532:	533:	534:	535:	536:	537:	538:	539:	540:	541:	542:	543:	544:	545:	546:	547:	548:	549:	550:	551:	552:	553:	554:	555:	556:	557:	558:	559:	560:	561:	562:	563:	564:	565:	566:	567:	568:	569:	570:	571:	572:	573:	574:	575:	576:	577:	578:	579:	580:	581:	582:	583:	584:	585:	586:	587:	588:	589:	590:	591:	592:	593:	594:	595:	596:	597:	598:	599:	600:	601:	602:	603:	604:	605:	606:	607:	608:	609:	610:	611:	612:	613:	614:	615:	616:	617:	618:	619:	620:	621:	622:	623:	624:	625:	626:	627:	628:	629:	630:	631:	632:	633:	634:	635:	636:	637:	638:	639:	640:	641:	642:	643:	644:	645:	646:	647:	648:	649:	650:	651:	652:	653:	654:	655:	656:	657:	658:	659:	660:	661:	662:	663:	664:	665:	666:	667:	668:	669:	670:	671:	672:	673:	674:	675:	676:	677:	678:	679:	680:	681:	682:	683:	684:	685:	686:	687:	688:	689:	690:	691:	692:	693:	694:	695:	696:	697:	698:	699:	700:	701:	702:	703:	704:	705:	706:	707:	708:	709:	710:	711:	712:	713:	714:	715:	716:	717:	718:	719:	720:	721:	722:	723:	724:	725:	726:	727:	728:	729:	730:	731:	732:	733:	734:	735:	736:	737:	738:	739:	740:	741:	742:	743:	744:	745:	746:	747:	748:	749:	750:	751:	752:	753:	754:	755:	756:	757:	758:	759:	760:	761:	762:	763:	764:	765:	766:	767:	768:	769:	770:	771:	772:	773:	774:	775:	776:	777:	778:	779:	780:	781:	782:	783:	784:	785:	786:	787:	788:	789:	790:	791:	792:	793:	794:	795:	796:	797:	798:	799:	800:	801:	802:	803:	804:	805:	806:	807:	808:	809:	810:	811:	812:	813:	814:	815:	816:	817:	818:	819:	820:	821:	822:	823:	824:	825:	826:	827:	828:	829:	830:	831:	832:	833:	834:	835:	836:	837:	838:	839:	840:	841:	842:	843:	844:	845:	846:	847:	848:	849:	850:	851:	852:	853:	854:	855:	856:	857:	858:	859:	860:	861:	862:	863:	864:	865:	866:	867:	868:	869:	870:	871:	872:	873:	874:	875:	876:	877:	878:	879:	880:	881:	882:	883:	884:	885:	886:	887:	888:	889:	890:	891:	892:	893:	894:	895:	896:	897:	898:	899:	900:	901:	902:	903:	904:	905:	906:	907:	908:	909:	910:	911:	912:	913:	914:	915:	916:	917:	918:	919:	920:	921:	922:	923:	924:	925:	926:	927:	928:	929:	930:	931:	932:	933:	934:	935:	936:	937:	938:	939:	940:	941:	942:	943:	944:	945:	946:	947:	948:	949:	950:	951:	952:	953:	954:	955:	956:	957:	958:	959:	960:	961:	962:	963:	964:	965:	966:	967:	968:	969:	970:	971:	972:	973:	974:	975:	976:	977:	978:	979:	980:	981:	982:	983:	984:	985:	986:	987:	988:	989:	990:	991:	992:	993:	994:	995:	996:	997:	998:	999:	1000:
-----	------	------	------	------	------	------	------	------	------	------	------	------	------	------	------	------	------	------	------	------	------	------	------	------	------	------	------	------	------	------	------	------	------	------	------	------	------	------	------	------	------	------	------	------	------	------	------	------	------	------	------	------	------	------	------	------	------	------	------	------	------	------	------	------	------	------	------	------	------	------	------	------	------	------	------	------	------	------	------	------	------	------	------	------	------	------	------	------	------	------	------	------	------	------	------	------	------	------	------	------	------	------	------	------	------	------	------	------	------	------	------	------	------	------	------	------	------	------	------	------	------	------	------	------	------	------	------	------	------	------	------	------	------	------	------	------	------	------	------	------	------	------	------	------	------	------	------	------	------	------	------	------	------	------	------	------	------	------	------	------	------	------	------	------	------	------	------	------	------	------	------	------	------	------	------	------	------	------	------	------	------	------	------	------	------	------	------	------	------	------	------	------	------	------	------	------	------	------	------	------	------	------	------	------	------	------	------	------	------	------	------	------	------	------	------	------	------	------	------	------	------	------	------	------	------	------	------	------	------	------	------	------	------	------	------	------	------	------	------	------	------	------	------	------	------	------	------	------	------	------	------	------	------	------	------	------	------	------	------	------	------	------	------	------	------	------	------	------	------	------	------	------	------	------	------	------	------	------	------	------	------	------	------	------	------	------	------	------	------	------	------	------	------	------	------	------	------	------	------	------	------	------	------	------	------	------	------	------	------	------	------	------	------	------	------	------	------	------	------	------	------	------	------	------	------	------	------	------	------	------	------	------	------	------	------	------	------	------	------	------	------	------	------	------	------	------	------	------	------	------	------	------	------	------	------	------	------	------	------	------	------	------	------	------	------	------	------	------	------	------	------	------	------	------	------	------	------	------	------	------	------	------	------	------	------	------	------	------	------	------	------	------	------	------	------	------	------	------	------	------	------	------	------	------	------	------	------	------	------	------	------	------	------	------	------	------	------	------	------	------	------	------	------	------	------	------	------	------	------	------	------	------	------	------	------	------	------	------	------	------	------	------	------	------	------	------	------	------	------	------	------	------	------	------	------	------	------	------	------	------	------	------	------	------	------	------	------	------	------	------	------	------	------	------	------	------	------	------	------	-------

***** 10/6/77 RUN #2 ***** PAGE 17
800,000,000 @eV HIGH INTENSITY PROTON SYNCHROTRON
S2 CONTINUED

25: BETA AT INPUT ENERGY = 0.42820776815
26: GAMMA AT INPUT ENERGY = 1.10658681953
27: BETA AT EXTRACTION ENERGY = 0.841821357162
28: GAMMA AT EXTRACTION ENERGY = 1.85268815628

ORBIT RADIUS = 7.00003139824
SYNCH DC AMP TURN = 72345.0814971
CHOKE DC AMP TURN = 72345.0814971
SAGITA = 0.9337970644472
SYNCH AC AMP TURN = 38628.8856726
CHOKE AC AMP TURN = 28499.5385872

\$ DC COIL COPPER = 333484.519311
COIL GAP WIDTH = 0.878411479569
CONDUCTOR WIDTH = 0.145496948871
\$ DC POWER = 451245.239203
CONDUCTOR HEIGHT = 0.2
JUMPER SEPARATION = 0.306450552891

63 \$ SYNCH. AC Cu = 83617.267464
COIL GAP WIDTH = 0.35
CONDUCTOR WIDTH = 0.0532252764455
\$ AC POWER = 108466.520845
CONDUCTOR HEIGHT = 0.2
JUMPER SEPARATION = 0.306450552891

\$ CHOKE AC Cu = 39911.709815
COIL GAP WIDTH = 0.226559814135
CONDUCTOR WIDTH = 0.0763131944944
CHOKE DC FIELD = 0.668589348403
\$ AC POWER = 123826.070041
COIL & GAP HEIGHT = 0.104665698226
COIL GAP LENGTH = 1.32757748641
CHOKE AC FIELD = 0.342171053583

\$ DC STEEL = 101724.257465
DC STEEL WIDTH = 1.46831319346
SYNCH AC STEEL W. = 0.503225276445
SYN AC Fe HEIGHT = 0.0664423067597
\$ AC STEEL = 125909.783317
STEEL LENGTH = 1.3744529494
CHOKE AC STEEL W. = 0.367186203124
CH. AC Fe HEIGHT = 0.114109457646

\$ FOR CAPACITORS = 41977.8714307
MAGNET AC ENERGY = 75625.2463923
CHOKE AC ENERGY = 29319.4321845 $\Sigma 10^5$ KVAR

S2 TOTAL COST 1489563.23789

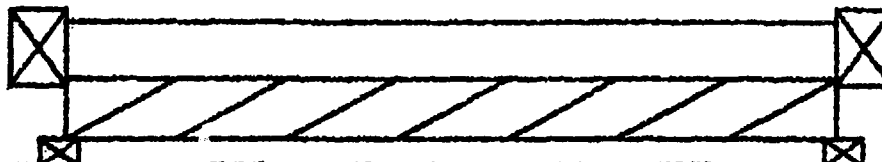
***** 10/6/77 RUN #2 ***** PAGE 18
900,000,000 GeV HIGH INTENSITY PROTON SYNCHROTRON
S2



S2 CROSS SECTION: CHOKE, SYNCHROTRON. (DASH=0.1 m.)



LENGTHWISE SECTION - SYNCHROTRON



LENGTHWISE SECTION - CHOKE

Power Supply and Ring Magnet Options
Walter Praeg
Argonne National Laboratory

Typical rapid cycling synchrotrons (RCS) have a biased sine wave magnet current and a nearly sinusoidal accelerating voltage together with an rf program for which the bucket area is nearly constant during the first part of the cycle. It has been proposed to introduce higher harmonic components into the magnet current waveform^{1,2}, or to use sinusoidal magnet currents of different frequencies in the half waves for the magnetic guide field² for the following beneficial affects:

1. The minimum of the magnet guide field can be flattened (front porch for injection).
2. The maximum \dot{B} is reduced during acceleration and hence, the maximum rf voltage/turn is reduced.
3. Lengthening of the guide-field rise time and shortening of the fall time improves the duty factor of acceleration.

Numbers 2 and 3 combined permit acceleration with fewer rf cavities. The reduction in total rf power is considerable, particularly at maximum \dot{B} , with a corresponding reduction in cost.

Figure 1 compares B and \dot{B} values for:

- single frequency excitation (f_o) —•—•—•—
- ac excitation with a 2nd harmonic ($f_o, 2f_o$) —————
- ac excitation with a 2nd and 3rd harmonic ($f_o, 2f_o, 3f_o$) —————

- two cases for excitation with different frequencies during acceleration and magnet reset.

The various excitation circuits and schemes for two rings, which utilize dipole magnets with cores common to both rings, will be discussed briefly.

1. One Ring 800 MeV - 16 GeV

1. 60 Hz Sine Wave

Only 50% of the wave is used for acceleration. A conventional phase controlled power supply can be used³ (36-or 48-phase system energized from the 60 Hz line). The rf-equipment is relatively expensive. The injection time is limited.

1.2 60 Hz Sine Wave Plus Harmonics

The peak value of B can be reduced by 33% if a second harmonic is added to the 60 Hz wave. This extends the acceleration time by about 26%.

The magnet voltage during reset is 30% higher than without harmonics. The voltages on the 2nd harmonic circuit components are relatively high (with the voltage on the 60 Hz magnet being 100%, the voltage on the capacitor is higher by a factor of 2.2, the voltage on the inductor by a factor 1.7). Reference 2 gives more details.

The control problem becomes twice as complicated as with a single frequency circuit.

Adding a 3rd harmonic compounds the above problems without improving the performance much (\dot{B} would be constant during most of the acceleration time). Figure 1 illustrates the waveforms for B and \dot{B} .

1.3 Dual Frequency Magnet Circuit

A 60 Hz repetition rate and a lower frequency magnet guide field during acceleration can be obtained as described in Reference 2. As illustrated in Figs. 1 and 2 the peak value of \dot{B} can be reduced by 33% or 40% by having guide fields during acceleration of 40 Hz or 36 Hz respectively, the corresponding frequencies for resetting the magnets are 120 Hz and 180 Hz.

In addition to reducing the cost of the rf system the lower frequency wave shape helps during injection.

Figure 3 shows general design curves for the dual frequency systems. A frequency f_1 during acceleration and a frequency f_2 during magnet reset result in a synchrotron repetition rate equal to frequency $f_o = 2 f_1 \times f_2 / (f_1 + f_2)$. Single frequency operation at f_o requires a capacitor bank C_o . The normalized curves f_1/f_o , f_2/f_o , f_2/f_1 , C_1/C_o and C_2/C_o in Fig. 3 illustrate the trade-offs between single (f_o) and dual frequency operation (f_1, f_2) as a function of f_o/f_1 .

The peak magnet voltage (during reset) is proportional to f_2 . It is apparent from Fig. 3 that this limits the ratio f_o/f_1 to values below 1.80. As f_o/f_1 increases the capacitance value of capacitor C_1 increases; however, the capacitor voltage, which is proportional to f_1

decreases. The opposite is true for the smaller capacitor bank C_2 the value of which decreases as f_0/f_1 increases, but with an ever higher voltage rating for capacitor C_2 and for switch S_1 which is proportional to f_2 .

By varying the timing of switch S_1 and/or the charge on capacitor C_1 before the switch is reclosed it should be possible to inject beam either into:

- a) a falling field ($B < 0$),
- b) an essentially flat field ($B \sim 0$),
- c) a slowly rising field ($B > 0$),
- d) a combination of a), b) and c).

1.3.1 Initial Operation at $f_1/2$, Future Upgrades to f_1 Followed by a 60 Hz Reposition Rate by Means of Dual Frequency Operation.

The synchrotron could be designed for a magnetic guide field of $f_1 = 36$ Hz during acceleration and 180 Hz to reset the magnets to achieve a 60 Hz repetition rate. The cost for the additional coil insulation for 180 Hz operation is only about 5% above the cost of 60 Hz magnets.

The dual frequency switched circuit lends itself to a staged sequence of synchrotron upgrades. For the initial stage, operating with a sinewave of $f_1/2 = 18$ Hz, only half of the rf cavities would be installed. For the second stage the capacitors would be reconnected for 36 Hz operation and the second half of the rf cavities be added. Finally the switching circuit and the higher voltage capacitor bank C_2

would be installed to operate at 60 pulses per second. Of course the initial stage could get by with even less rf-power and ring magnet excitation if the synchrotron energy, with a 18 Hz sinusoidal magnetic guide field, would be less than 16 GeV.

2. Two Rings (booster 0.8-5 GeV, synchrotron 5-16 GeV)

2.1 One Power Supply for Both Rings.

The two rings must be 180° out of phase. Therefore, their energy can be transferred from one to the other via a resonant capacitor bank (one ring acts as a choke for the other as in a conventional biased circuit); this eliminates the costs for chokes and only one capacitor bank is required. With reference to Fig. 4 the currents are

$$i_1 = I_{dc} - I_{ac} \sin \omega_0 t \quad (1)$$

$$i_2 = I_{dc} + \frac{L_1}{L_2} I_{ac} \sin \omega_0 t \quad (2)$$

$$i_c = -\frac{L_1 + L_2}{L_2} I_{ac} \sin \omega_0 t \quad (3)$$

$$\omega_0 = \left(\frac{L_1 + L_2}{L_1 L_2 C} \right)^{1/2} . \quad (4)$$

Ring 1 accelerates between times a and b, ring 2 between times a^1 and b^1 . It will take a little effort to design the rings for minimum overall cost.

2.2 Two Rings on a Common Core

Probably the least expensive two-ring circuit may be the one illustrated by Fig. 5. This system is a modification of the one described in Reference 4, which places an ac magnet (having only top and bottom yokes⁵) inside a dc magnet. Like the circuit described in Section 2.1 above, it does not require a separate choke. In addition, it has the following desirable features:

1. The inductances of the two rings are connected in series. Therefore, the circuit needs only about 25% of the tuning capacitance required by the conventional circuit of Fig. 4.
2. No dc current flows through the ac ring magnet coils.
3. No ac current flows through the dc coil.
4. The dc circuit couples to the ac circuit. However, the net voltage induced in the ac coils when the dc circuit is first energized is relatively small.
5. The ac circuit is not coupled to the dc circuit.

This two-ring magnet design may also be the least expensive to build. The beams in the two rings go in opposite directions.

A second harmonic may be added if we use laminated iron and add a 120 Hz excitation coil that surrounds the two 60 Hz coils. Figure 6a illustrates such an arrangement; for sake of simplicity two identical rings are shown. One dc coil provides a bias for both gaps. Since the 120 Hz circuit is coupled to the dc circuit a 120 Hz parallel tuned circuit is part of the dc circuit to reduce the induced 120 Hz current. Again the 60 Hz circuit does not couple to the dc or the 120 Hz circuit. The second harmonic reduces \dot{B} during acceleration by approximately 33%. However, it also makes the rising field portions approximately 28% longer (10.7ms vs. 8.3 ms). One might, therefore, accelerate in the booster for a shorter time (8.5 ms) then in the synchrotron (10.7 ms). Figure 6b illustrates the waveforms.

For an actual booster and synchrotron combination the gaps in the two rings would be different and similar to the ones indicated in Fig. 5.

References

1. W. Hardt and D. Moehl, "A Method of Reducing the Phase Oscillation Frequency in a Fast Cycling Synchrotron," CERN, IRS-300/GS/68-3, Geneva, January 31, 1968.
2. Foss, Praeg, "Shaped Excitation Current for Synchrotron Magnets" IEEE Transactions on Nuclear Science, Vol. NS-28, No. 3, June 81.

3. Praeg, McGhee, "Ring Magnet Power Supply for a 500 MeV Synchrotron, "Conference Record Industry Application Society, IEEE-IAS-1978, 13th Annual Meeting, Toronto, Oct. 1978.
4. Burke, Foss, "A Rapid Cycling Synchrotron Magnet with Separate AC and DC Circuits," IEEE Transactions on Nuclear Science.
5. Praeg, "Pulsed Magnet Systems for High Energy Physics Beam Lines, "Proceedings of 5th International Conference on Magnet Technology, Rome, Italy, April 75.
6. Praeg, McGhee, Volk, "Phase Lock of Rapid Cyclic Synchrotron and Neutron Choppers," IEEE Transactions on Nuclear Science, Vol. NS-28, No.3, June 81.

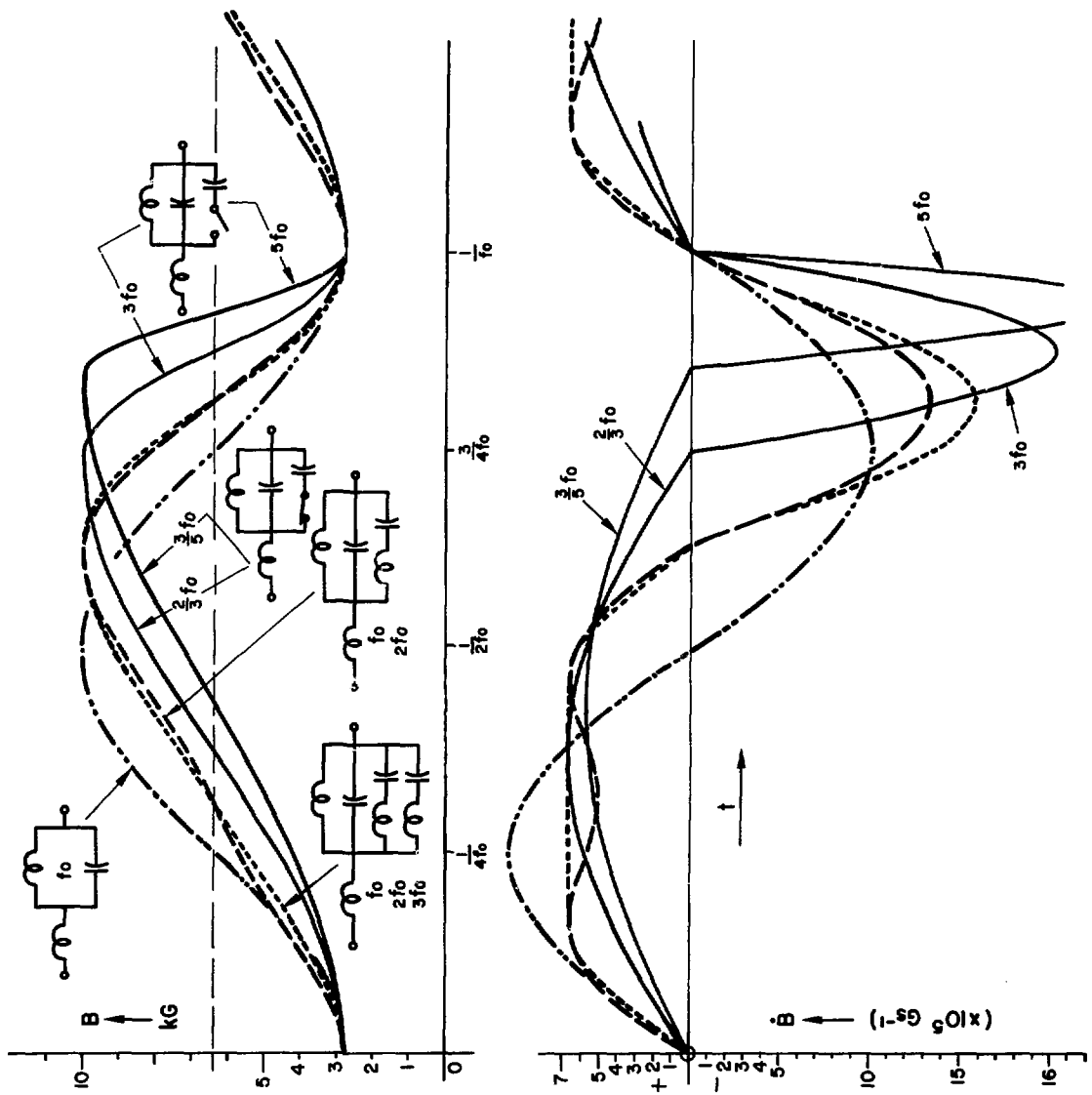


Fig. 1 B and B^* values for various magnet excitations.

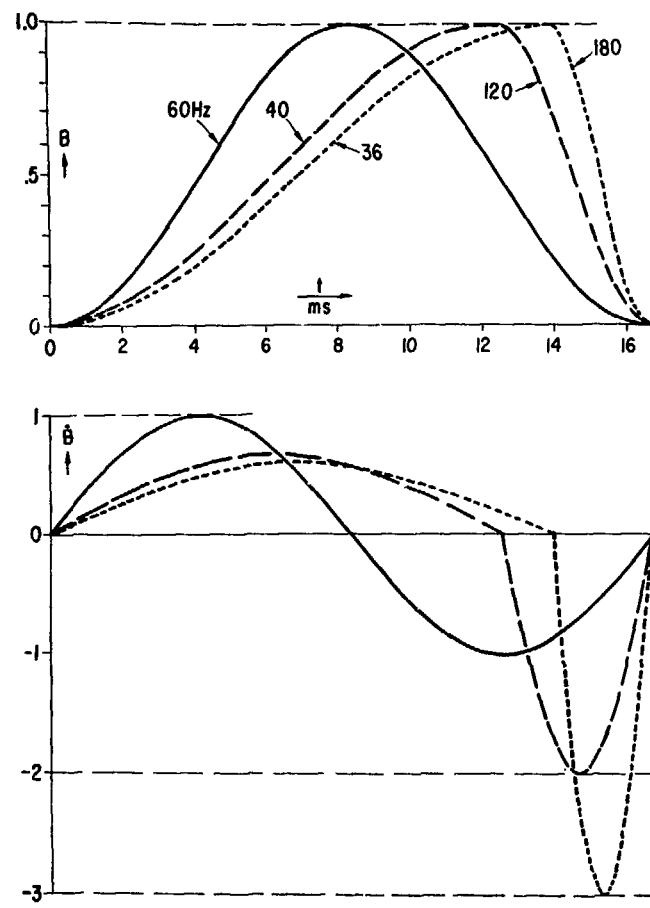


Fig. 2 Single and dual frequency excitation for a 60 Hz repetition rate.

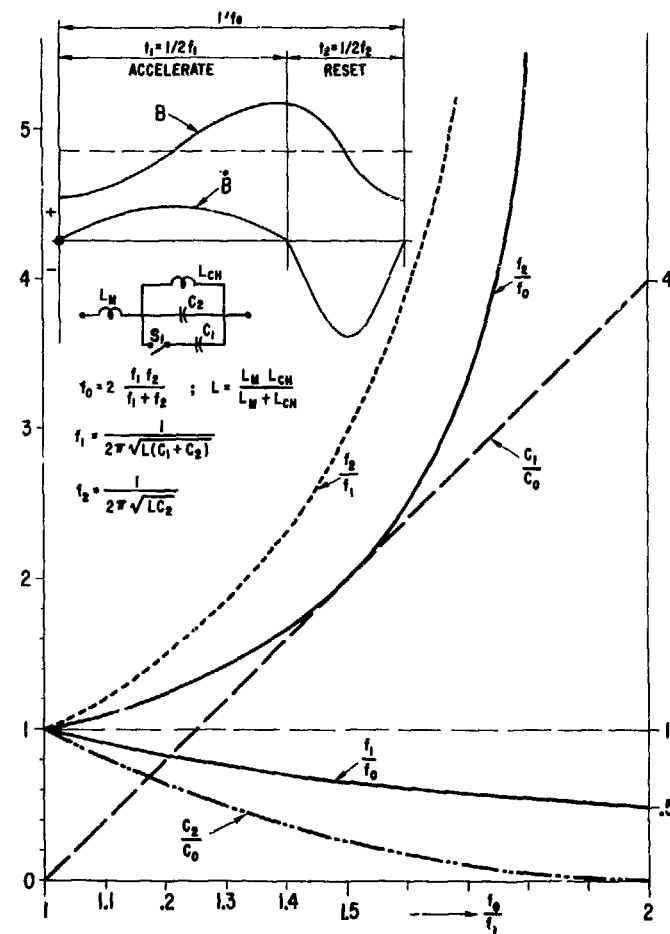


Fig. 3 General design curves for the dual frequency circuit.

Fig. 4 Resonant circuit for two rings with one common power supply.

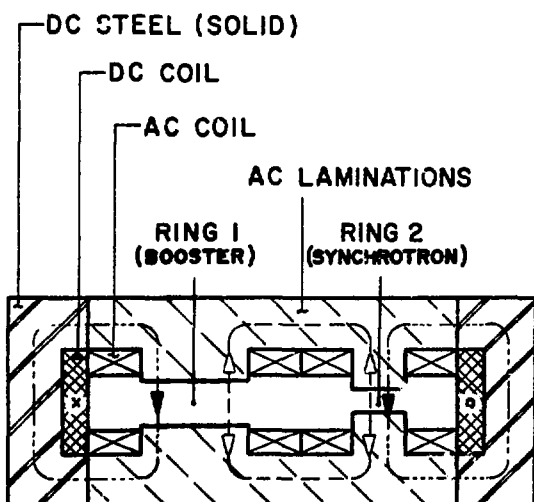
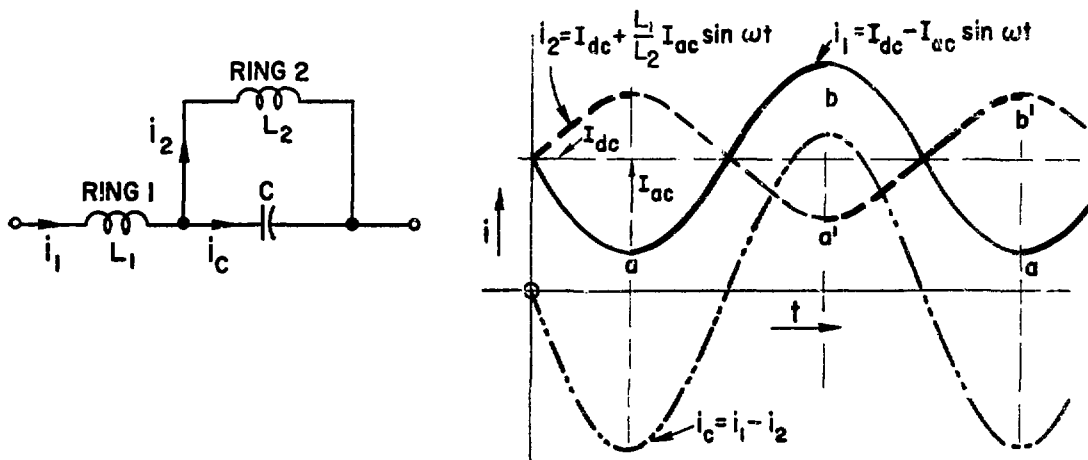


Fig. 5 Two rings utilizing one core.

Equivalent circuit.

Fig. 6 Two rings utilizing one core and 2nd harmonic to reduce B .

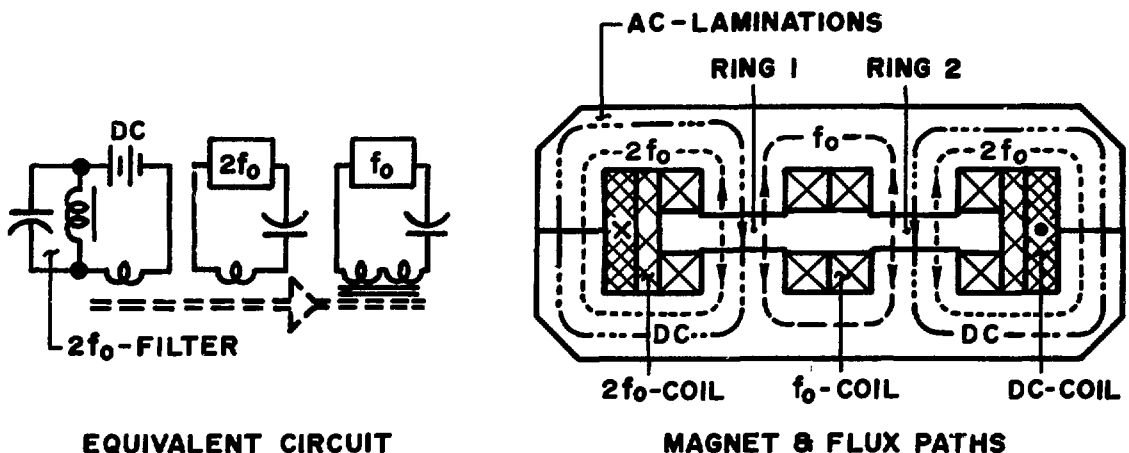


FIG.6a TWO-RINGS WITH COMMON WINDINGS, CORE, & POWER SUPPLIES.

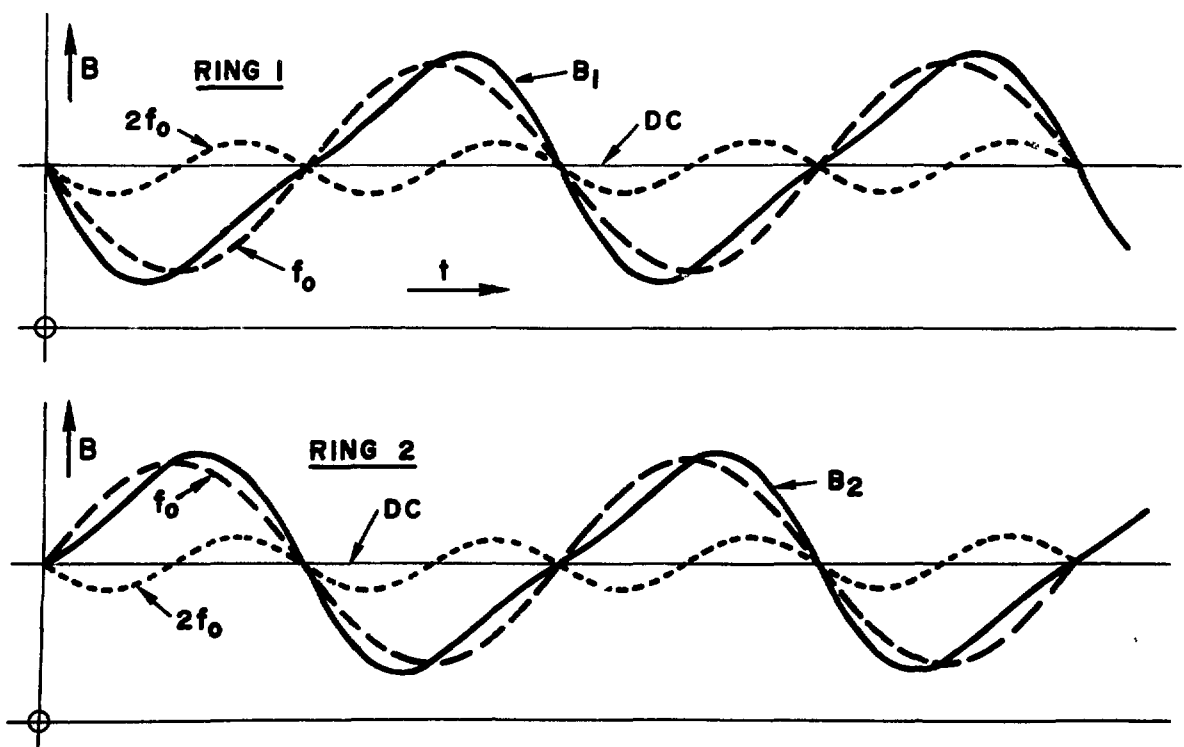


FIG. 6b FLUXES IN TWO-RING CORE WITH FIRST (f_0) AND SECOND ($2f_0$) HARMONIC AND DC EXCITATION.

NOTES FOR A KAON FACTORY DESIGN

Grahame H. Rees and Richard K. Cooper

1. Introduction

Two earlier Kaon Factory designs have been suggested: R. R. Wilson (1) and L. C. Teng (2). Both were based on proton beams of average current 100 μ A, derived from LAMPF at 800 MeV and accelerated to kinetic energies up to 16 GeV. Since these earlier designs the experimental requirements have been further specified to include the provision of sub-nanosecond bunches at a bunch repetition frequency of approximately 50 MHz.

In reference 1 a staged development was proposed with an initial construction of a rapid cycling 2-4 GeV proton synchrotron. Subsequently a slow-cycling 8 GeV conventional proton synchrotron was to be added and later still a 16 GeV (or higher) slow-cycling superconducting ring. All rings were to be included in the same tunnel, of mean radius \sim 30 m. The slow-cycling rings would accept up to 100 pulses from the fast-cycling ring.

In reference 2 a 16 GeV fast-cycling proton synchrotron was proposed, housed in the same tunnel as a 16 GeV stretcher ring. The mean radius proposed was 122 m and the purpose of the stretcher ring was to provide a good duty cycle via a slow-extracted 16 GeV beam.

The requirement of sub-nanosecond proton bunches has implications for the entire design. It is not practical to obtain such bunches for the small size rings and large beam currents of the scheme of reference 1. The choice of synchrotron mean radius, magnet lattice, and RF schemes are all-important. To reduce the RF system requirements it is an advantage to approach the transition energy of the lattice at the energy chosen for slow extraction. Thus for slow extraction at 16 GeV where $\gamma = 18.053$, an appropriate choice for gamma transition is $\gamma_t = 19$. This choice has the added advantage that transition is not crossed during acceleration. The value of γ_t may be compared with that for the lattice of reference 2, where $\gamma_t \sim 8$.

The basic scheme of reference 2 is adopted in this note but significant changes are proposed for the mean radius, for the magnet lattices of the synchrotron and stretcher ring, and for the RF schemes. A maximum frequency

of 48 MHz is chosen for the RF system in the synchrotron, but a frequency 7 or 8 times larger is chosen for the stretcher ring to provide further bunch compression.

Brief notes are given of the features considered most important for the initial design of the Kaon Factory.

2. List of Important Aspects of the Kaon Factory Design

Choice of gamma transition and magnet lattices.

Choice of magnet guide field waveform.

Basic RF parameters for synchrotron and stretcher ring.

Transverse space charge effects.

Synchrotron injection at 800 MeV.

Transfer at 16 GeV from synchrotron to stretcher ring.

Slow extraction from stretcher ring at 16 GeV.

Beam loss.

Correction elements.

Instabilities.

Cost optimization of design.

Future developments.

3. Choice of Gamma Transition and Magnet Lattices

The total voltage on the RF cavities to provide a defined equilibrium bunch length is proportional to $n \equiv |\gamma^2 - \gamma_t^2|$. Hence the choice of $\gamma_t = 19$ for $\gamma = 18.053$. It is not an advantage to have a smaller value of n , for the phase oscillation frequency also decreases and there is then insufficient time in acceleration to achieve the equilibrium bunch length.

Gamma transition is approximately equal to the horizontal betatron tune Q_h for the case of a simple lattice. A large value of γ_t thus infers large focussing and a large number of cells in the magnet lattice; for example, 76 cells are required for $Q_h = 19.2$ if the phase shift per cell, μ , equals $\sim \pi/2$.

A simple lattice is not proposed, however, for either the fast-cycling synchrotron or the stretcher ring. The synchrotron has, during early acceleration, a high value of synchrotron tune, Q_s , because of the rapid rate of rise of the guide field and because of the choice of a 40-48 MHz RF system. To minimize the resulting betatron-synchrotron coupling, the RF cavities should be located in regions of zero dispersion, $n(s) = n'(s) = 0$. This location suggests the use of a missing-magnet separated function lattice or the use of a lattice with matched insertions. Both may provide long straight sections, advantageous for localizing RF systems and for locating injection systems, ejection systems, and beam-loss protection systems. A missing-magnet lattice is preferred for the synchrotron while one with matched insertions is preferred for the stretcher ring. As it is desired to locate the stretcher ring vertically above the synchrotron, identical normal lattice cells are chosen for the arcs which link the long straight sections.

A special matched insertion is proposed for the stretcher ring which has high values of β_h and low values of β_v in the center section of the insertion. Such a feature is designed to increase the efficiency of a slow extraction system.

For the normal cells of the lattice a choice may be made between FODO-type cells (FBDB), doublet cells (DFB), or triplet cells (FDFB). An initial choice has been made for the doublet cell; it provides a longer bending length than the FBDB cell and it has lower quadrupole gradients than the triplet cell. Further study may lead to a revision of this choice.

The number of superperiods is made 4. In the missing magnet design of the synchrotron, each superperiod has 24 cells. Of these, 14 are normal cells, 6 are free of bending magnets and at each end of the 14 normal cells there are 2 cells with bending magnets of reduced length or strength (to provide the dispersion-free straight region):

$$(DFOB_1)(DFB_20)(14DFB)(DFOB_3)(DFB_40)(6DFO)$$

The only difference in the stretcher ring lattice is that the 6 DFO cells in each superperiod are replaced by a matched insertion of central symmetry.

The phase shift per cell is approximately $\pi/2$, with the synchrotron tunes approximately 23.25. These tunes are adequately spaced from superperiod resonances up to order 3. In the stretcher ring the aim is to have

$Q_v = 23.25$, but the large β_h values will lead to a lower horizontal tune. The stretcher ring insertion is to be designed to make $Q_h = 21.33$, that is $30_h = 64$, a suitable resonance for slow extraction. The major part of the dispersion exists in 16 cells of each superperiod; the contribution to the tunes from these is approximately 15.5, and the expected value of γ_t is then $15.5\sqrt{(24/16)} \sim 19$.

The doublet cell provisionally selected is:

Cell length	9.3 m
Quadrupole lengths	0.75 m
Dipole length	5.3 m
D to F quadrupole spacing	1.0 m
F to D quadrupole spacing	6.8 m
Quadrupole-dipole separation	0.75 m
Quadrupole gradient at 16 GeV	31.4 T m^{-1}
Maximum dispersion η	0.65 m
Maximum β	14.18 m
Maximum β in dipole	11.57 m

The strong focussing results in low values of η and β and hence small magnet apertures. The mean radius that results from 96 cells of length 9.3 m is 142.09353 m.

The synchrotron transverse space charge forces dictate transverse emittance values (phase space area π) of $\epsilon \sim 10 \mu\text{rad m}$. This value is larger than the value assumed in references 1 and 2 to allow for the rapid initial bunching of the beam during acceleration. The stretcher ring may have a much smaller value of ϵ_v ; the exact value for the stretcher ring apertures will depend on a detailed study of slow extraction.

Maximum vertical betatron amplitudes in the synchrotron are:

Quadrupole (D)	11.9 mm
Dipole	10.8 mm

To these values should be added an allowance for closed orbit deviation; e.g. a vertical half-aperture of 20 mm corresponds to a vertical acceptance area of $28\pi \mu\text{rad m}$.

The length of straight sections in the 4 x (6DFO) cells is 163.2 m.

The missing-magnet insertion is preferred for the synchrotron in preference to a special matched insertion for two reasons:

- a. There results very little mismatch under space charge conditions, and
- b. It allows the quadrupoles to be standardized and so simplifies the resonant magnet power supply.

4. Choice of Magnet Guide Field Waveform

A magnet repetition frequency of 60 Hz and an average beam current of 100 μA corresponds to 1.04×10^{13} protons per pulse and to the quoted transverse emittances, for space charge reasons, of $\pi e = \pi 10 \mu\text{rad m}$. A lower repetition frequency leads to more protons per pulse, larger magnet apertures, enhanced beam loading, and prospects of instability, but a reduced number of RF cavities. If the magnet guide field waveform is a 60 Hz sine wave the peak RF volts needed at mid-cycle is approximately 10 MV. This value corresponds to a large number of tuned RF cavities, about 100. The peak volts needed just prior to extraction is less than half this value for the choice of $r_t = 19$ and the longitudinal bunch emittances defined in section 5 of this note. A reduction in peak RF volts may thus be realized by the use of a modified guide field waveform. Two schemes to provide such a modified waveform are described in reference 3 which lead to a reduction in peak RF volts of ~ 30 percent. In one scheme a second harmonic resonant magnet current is added to a fundamental component to reduce the peak value of dB/dt in acceleration. The second scheme employs switching circuits to give a sharper fall time than rise time for the guide field.

In addition to aiding the RF system design a modified waveform for the guide field helps in the 800 MeV injection process and also in minimizing transverse space charge forces. Ideally, a flat-bottom to the guide field is required for injection (see section 7), but close tolerances are required if synchronous injection is employed.

5. Basic RF Parameters for Synchrotron and Stretcher Ring

The RF volts vary through the magnet cycle and are a function of dB/dt , of the longitudinal bunch emittance, and of the desired bunch length. In early acceleration a long bunch length is an advantage to reduce the transverse space charge forces. Late in the synchrotron cycle the bunch length must be reduced to ~ 1 ns to allow efficient transfer into the RF buckets created by the higher frequency RF system of the stretcher ring. After transfer, the RF volts must be increased adiabatically in the stretcher ring to reduce the bunch length.

The initial longitudinal bunch emittance is assumed to be:

$$\int \Delta E / h\omega \, d\phi = 0.058 \text{ eV sec} ,$$

where ω is the angular frequency of circulation of the protons, and h is the harmonic number ($= \omega_{rf} / \omega$). The input $\Delta p/p$ from LAMPF is taken to be $\pm 10^3$ and the area assumed is that after bunch capture. Some dilution will occur during acceleration and the bunch area at 16 GeV is taken as 0.1 eV sec. The linac bunch frequency is 201.25 MHz and the synchrotron start frequency is taken at one-fifth this value, 40.25 MHz. The final frequency at 16 GeV is then 47.742 MHz. A harmonic number of 14 corresponds to a mean radius of 141.7025 m. Note that this radius is slightly different from that of section 3.

As an example of RF parameters, approximate values are given for:
A sine wave guide field of repetition frequency 60 Hz,
A transition energy for both lattices of $\gamma_t = 19$:

$t(\text{ms})$	β	ϕ_s	Synchrotron Peak RF Volts	Bunch Duration
0	.84181	0°		
1	.90579	39°	5.0 MV	8.58 ns
2	.96595	55°	7.2 MV	5.92 ns
3	.98759	60°	8.9	3.25 ns
4	.99424	60°	9.9	2.2 ns
4.1667	.99483	60°	9.9	
5	.99673	60°	9.4	1.75 ns
6	.99780	60°	7.6	
7	.99828	40°	6.4	1.0 ns
8.3333	.99850	0°	3.0	1.0 ns

The peak voltage at time $t = 0$ requires a detailed study of the trapping process. The voltages given for $t = 1$ and $t = 2$ ms correspond to full buckets; this minimizes the transverse space charge forces. At 16 GeV, the 3.0 MV corresponds to an equilibrium bunch length of 1 ns. Tracking studies will indicate how close to this value the actual bunch length becomes.

If the stretcher ring has an RF frequency of 7×47.472 MHz the RF voltage for bucket matching is $\sim 3/7$ MV. The voltage to reduce the bunch to $1/2$ ns is ~ 7 MV. The voltage to reduce the bunch to $1/3$ ns is ~ 35 MV. The synchrotron tune Q_s is close to 0.1 at time $t = 1$ ms but drops to .045 at $t = 2$ ms and .015 at $t = 3$ ms. AT 16 GeV, $Q_s \sim .002$. The high initial Q_s has implications for betatron-synchrotron coupling and is the motivation for providing the dispersion-free straight sections.

RF Cavity Design – drift tube cavities

- May be necessary to use $< \lambda/2$ units.

6. Transverse Space Charge Forces

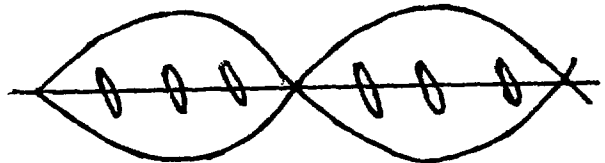
Maximum space charge detuning in early acceleration.
 B_{BY}^2 minimum gives this condition.
 Check that higher space charge does not exist in synchronous injection.

7. Synchrotron Injection

H- 10 mA for 160 μ s

a) Synchronous 48.25 MHz buckets 60 percent duty cycle
Debunching linac bunches? What is momentum distribution in bucket? Problems
to study. Motion at edge of bucket. Estimate of transverse space charge.
Tolerances for synchronization.

$$\frac{\Delta\omega}{\omega} = \eta \frac{\Delta B}{B} \sim \frac{1}{4} \frac{\Delta B}{B}$$



$$\frac{\Delta B}{B} = \frac{4\Delta\phi/\tau}{2\pi 40.25 \times 10^6} = 15 \times 10^{-6}$$

where τ = total injection time

$\Delta\phi$ = synchronization tolerance = $\pi/20$

b) Alternative is to debunch beam first during injection; then switch on RF.
Possible advantages - transverse space charge forces appear later. Disad-
vantages - trapping losses. Since longitudinal space charge forces are
relatively low the trapping efficiency may be high - tracking studies needed.

8. Transfer at 16 GeV from Synchrotron to Stretcher Ring

Fast extraction from Synchrotron:

- a) 15 ns rise time fast kicker and septum magnet.
- b) Dump 1 or 2 bunches at low energy gives slower rise time for fast kicker at high energy.

50 ns rise - spark gap vs thyratron switches - reliability at 60 Hz.

Vertical Extraction

Horizontal Injection

SHAPED EXCITATION CURRENT FOR SYNCHROTRON MAGNETS*

M. Foss and W. Praeg
Argonne National Laboratory
Argonne, IL 60439

Reference 3

Summary

A 500 MeV synchrotron at Argonne National Laboratory (ANL) operates at 30 Hz with its beam spill locked to neutron choppers with a precision of ± 0.5 μ s. The average beam will be increased by running the magnets at 45 Hz. Three 45 Hz circuits are discussed which differ greatly in overall cost and complexity.

The first is a conventional 45 Hz sine wave circuit. The reduction in time for beam acceleration results in a costly increase in peak RF power. This problem is avoided in the other two circuits by making the field rise slowly and fall rapidly.

The second circuit discussed is resonant at 45 Hz and 90 Hz. Exciting this circuit with a mixture of dc, 45 Hz, and 90 Hz can produce a magnetic field with the same maximum dB/dt as the present 30 Hz field.

A third, and possibly least expensive, solution is a novel circuit which produces 30 Hz during acceleration and 90 Hz when the magnets are reset. The RF requirements are, of course, identical to present requirements during acceleration. Circuit details are given.

Introduction

The ring magnets of the 500 MeV Rapid Cycling Synchrotron (RCS) at ANL are excited with a dc bias of 2300 A modulated by a 30 Hz sine wave of 1300 A peak. An economical way to generate this current is with a 24-phase programmed power supply energizing a 30 Hz resonant circuit as shown in Fig. 1. The ring magnet is $L_M = 28.8$ mH, the choke $L_{CH} = 16$ mH and the condenser $C = 3000 \mu$ F. The circuit losses are 475 kW and the power supply voltage is $e = 137$ V - 238 V sin $188.5t$.

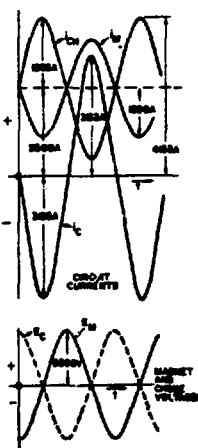
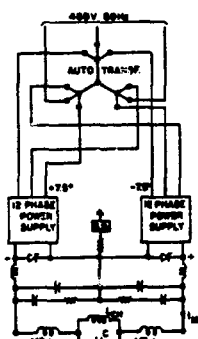


Fig. 1. Ring magnet power supply and waveforms of resonant circuit.

To increase the average beam, we will run the RCS at 45 Hz. Three magnet circuits employing three different magnet current wave shapes are presented.

45 Hz Sine Wave Magnet Excitation With New RF

The simple change to make in the magnet circuit is to tune the circuit for 45 Hz and drive it with a 45 Hz sine wave. The resonant circuit components are:

L_M	$= 22.8$ mH	R_M (DC)	$= 44$ m Ω
L_{CH}	$= 80$ mH	R_{CH} (DC)	$= 36$ m Ω
C	$= 705 \mu$ F	R_C (45 Hz)	$= 23$ m Ω
Power	$= 550$ kW	Peak Volts	$= 385$ V

This circuit could be driven with our present power supply. The capacity required is much smaller, but the operating voltage is 50% larger. If the same condensers are used, we will require two in series by two in parallel or a total condenser requirement of 2820μ F. This plan calls for a new choke.

Unfortunately, the more rapid rise of the magnetic field is associated with much larger peak RF power requirements to accelerate the proton beam. The cost of the RF makes this magnet circuit unattractive. The circuits presented below avoid this problem.

45 Hz-Plus 90 Hz Magnet Excitation

The RCS can operate without increasing the RF peak power if the maximum dB/dt is not increased. This is accomplished with a wave form using two harmonics:

$$B = \frac{B_{\max} + B_{\min}}{2} + \frac{B_{\max} - B_{\min}}{2} \times$$

$$\left[\frac{B/10}{27} \sin(2\pi 45t) + \frac{5}{27} \sin(2\pi 90t) \right]$$

The shape of B versus t is the same as the shape of I_M versus time in Fig. 2a. The field is maximum or minimum when $\cos(2\pi 45t) = 1/10$ and the slope has two maxima where $\cos(2\pi 45t) = -2/10$. The proposed two-harmonic circuit and the current waveforms are also shown in Fig. 2a. The voltage waveforms are shown in Fig. 2b and the impedance versus frequency in Fig. 2c. The values for the circuit elements are:

L_M	$= 22.8$ mH	R_M (DC)	$= 44$ m Ω
L_1	$= 80$ mH	R, L_1 (DC)	$= 20$ m Ω
L_3	$= 35$ mH	R, L_3 (45 Hz)	$= 50$ m Ω
C_2	$= 357 \mu$ F	R, C_2 (45 Hz)	$= 45$ m Ω
C_3	$= 176 \mu$ F	R, C_3 (45 Hz)	$= 90$ m Ω
Power	$= 500$ kW	Peak Volts	$= 514$ V

As with the single harmonic circuit above, the voltage on C_2 makes it necessary to use two condensers in series and two in parallel if the available condensers are used. The voltage on C_3 is even larger so that four in series and four in parallel are required. The total, using existing condensers, is 4250μ F. The major problem with this circuit is that the control problem becomes twice as complicated. This is shown schematically in Fig. 2d. Direct current must be regulated, as well as current and phase of each harmonic. The magnet circuit must be kept tuned to both 45 Hz and 90 Hz or the kVA will become excessive. Not only are there more factors to control, but also a precise control of the relative phase of the 45 Hz and 90 Hz is necessary to maintain the injection field and phase lock with the neutron chopper. The additional circuit losses make it necessary to add a third power supply. This allows one to more accurately produce the voltage wave shown in Fig. 2b with rectifier phase control. A 36-phase rectifier

system is obtained by shifting, with an auto transformer, the 3-phase, 460 V input of two of the three identical 12-phase power supplies by $\pm 100^\circ$.

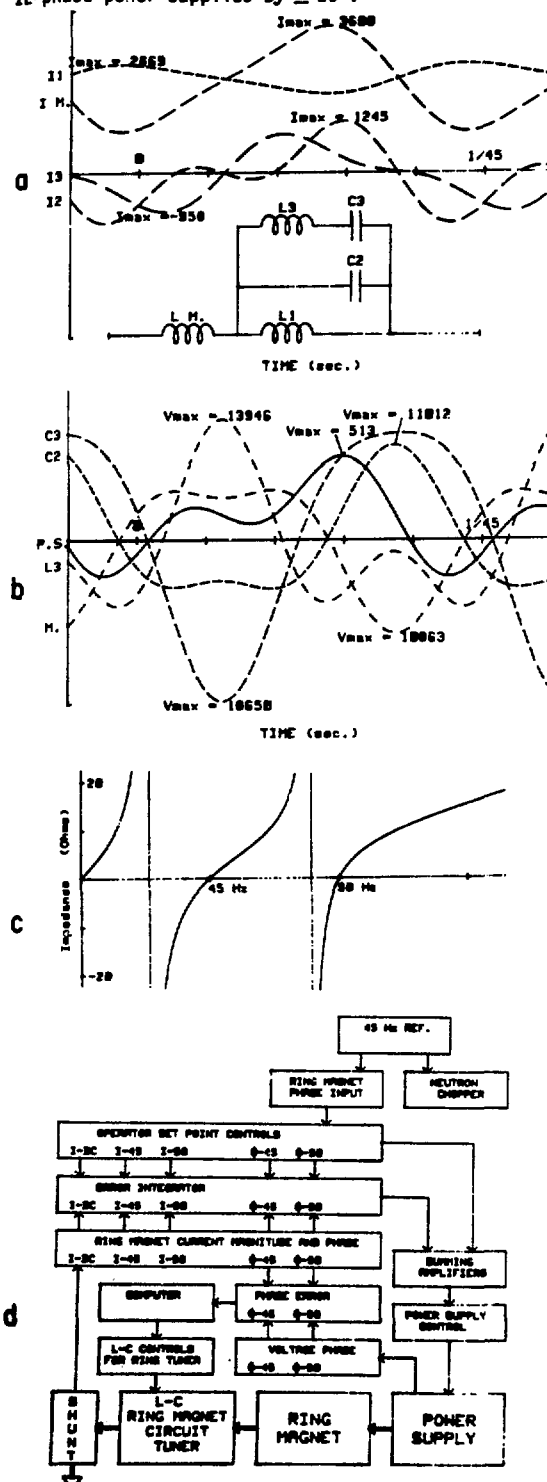


Fig. 2. 45 Hz plus 90 Hz excitation.

Accelerate With 30 Hz and Reset Magnet With 90 Hz

We nearly can have our cake and eat it with a third solution. During proton acceleration the synchrotron operates at 30 Hz utilizing the existing RF equipment. A repetition rate of 45 pps is achieved by resetting the magnet with a 90 Hz half sine wave. During this time, the RF is shut off. The magnet and capacitor voltage will increase during reset by a factor three. This is within the rating of the magnet and choke.

Figure 3 illustrates the circuit. At injection, switch S_1 is closed and the currents and voltages oscillate at 30 Hz. At the end of acceleration, the current in the capacitors is at its peak value. However, the energy in the capacitors is zero. If we now disconnect capacitor C_2 , the circuit will reset with a 90 Hz half sine wave. During the reset, the peak voltage on capacitors C_1 exceeds the peak voltage during acceleration by a factor three. A new relatively small capacitor bank C_1 , rated 12 kV rms, must be purchased. The solid state switch S_1 operates when:

- the current is at its peak,
- the voltage across it is practically zero,
- the forward voltage builds up at a rate of $dv/dt \leq \omega E \leq 565s^{-1} \times 16.8 \text{ kV} \leq 9.4 \text{ V}/\mu\text{s}$ which is negligible.

The capacitor current in C_2 is zero when the switch closes at the end of the 90 Hz half cycle, and not at its peak value as required by the 30 Hz resonant circuit. This will cause a small transient because switching is done with very little transfer of energy; it requires not many amperes seconds to get a few kA into capacitors which are near zero voltage. Operation of the switch (repeatability, time jitter, etc.) is most critical before injection. Therefore, the switch should be closed shortly before the 90 Hz operation ends. It should be relatively easy to protect against circuit malfunctioning:

- If the switch fails to open, the circuit will complete its 30 Hz "low voltage" cycle.
- After a few 30 Hz cycles the RCS is again in phase with the 45 Hz chopper and the 30 Hz and 90 Hz operation can be resumed.

Switch S_1 is a bidirectional solid-state switch made from back-to-back SCR assemblies, SCR_1 and SCR_2 , shown in Fig. 4. As seen in Fig. 3, a negative step change of capacitor current is initiated at time t_0 when SCR_1 is turned on. A quarter of a 30 Hz cosine wave later, this current is zero and SCR_1 turns off. At time t_1 , a 0.5 ms long gate signal turns on SCR_2 and a positive sinusoidal current charges capacitor C_2 . At time t_2 , after a quarter of a 30 Hz sine wave, the capacitor voltage is zero and the capacitor current is at its maximum. At this time a turn-off circuit brings the current through SCR_2 to zero taking capacitor C_2 out of the circuit.

Circuit Description

For $t_0 < t < t_1$ and $t = t_2 + \dots$ As shown in Fig. 4a, SCR_1 is turned on and the choke current discharges at 30 Hz through the magnets and the parallel connection of C_1 , C_2 , and C_x . (Drawing the capacitor symbol in heavy lines indicates charge on the capacitor.)

At $t = t_1$ (Fig. 4b) -- The capacitor current goes through to zero ($i_{C_2} = i_{CH}$) and SCR_1 turns off. The capacitors are at 5.6 kV.

At $t_1 < t < t_2$ (Fig. 4c) -- With SCR_2 turned on, the capacitor current reverses.

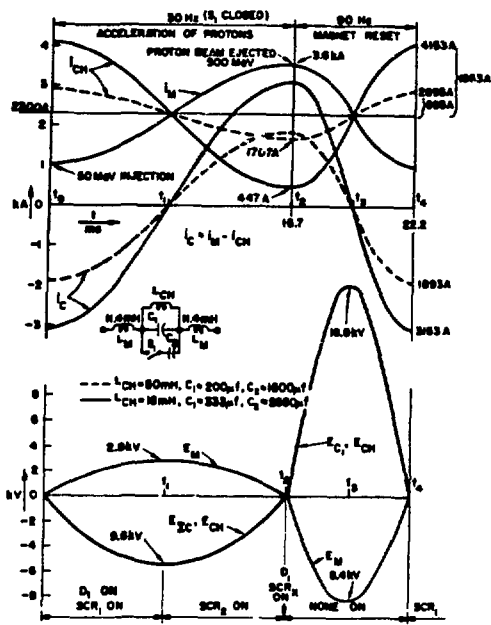


Fig. 3. Waveshapes for acceleration at 30 Hz and reset at 90 Hz.

At $t = t_2$ (Fig. 4d) -- The capacitor current is at its peak; the capacitors are discharged. At this time, SCR_x is turned on. This provides discharge paths for turn off capacitor C_x via SCR_x , SCR_2 , and C_2 (current i_x') and via SCR_x , L_x , and C_1 (current i_x'').

At $t = t_2 + 25 \mu s$ (Fig. 4e) -- The reverse current i_x' has turned off SCR_2 . A resonant discharge of C_x via SCR_x , L_x , and C_1 continues for 80 μs (6.25 kHz).

At $t = t_2 + 80 \mu s$ (Fig. 4f) -- The charge on C_x has reversed, i_x'' is zero and SCR_x turns off. In the next 80 μs capacitor C_x will reverse its polarity via C_1 , L_x , and D_x . This charge, shown in Fig. 4g, remains on C_x because SCR_x is turned off and D_x blocks discharge. Thereafter, the solid state components will carry no current until $t > t_4$.

At $(t_2 + 160 \mu s) < t < t_4$ (Figs. 4g, 4h, 4i) -- The circuit resonates at 90 Hz. At $t = t_3$ the voltage on capacitor C_1 is at 90 kV and its current is zero. At $t = t_4$, the voltage on C_1 is zero and its current is at its peak. To assure a smooth transition from 90 Hz to 30 Hz operation at time t_4 , a 0.5 ms gate signal is applied to SCR_1 0.1 ms before t_4 .

In the circuit of Fig. 4 only ac currents are shown. For sake of clarity we have not shown a saturable time delay reactor to limit di/dt during turn-on of SCR_x ; such a reactor may also be required to protect SCR_2 in case it turns on accidentally when C_1 is at a high voltage ($t=t_3$). Of course, other turn off circuits may be used. For example, capacitor C_x could be connected between the anodes of SCR_2 and SCR_x and charged from an independent low voltage dc supply; in this case, diode D_x is not required.

Reference

1. W. Praeg, D. McGhee, G. Volk, "Phase Lock of Rapid Cycling Synchrotron and Neutron Choppers," (Proceedings of this conference).

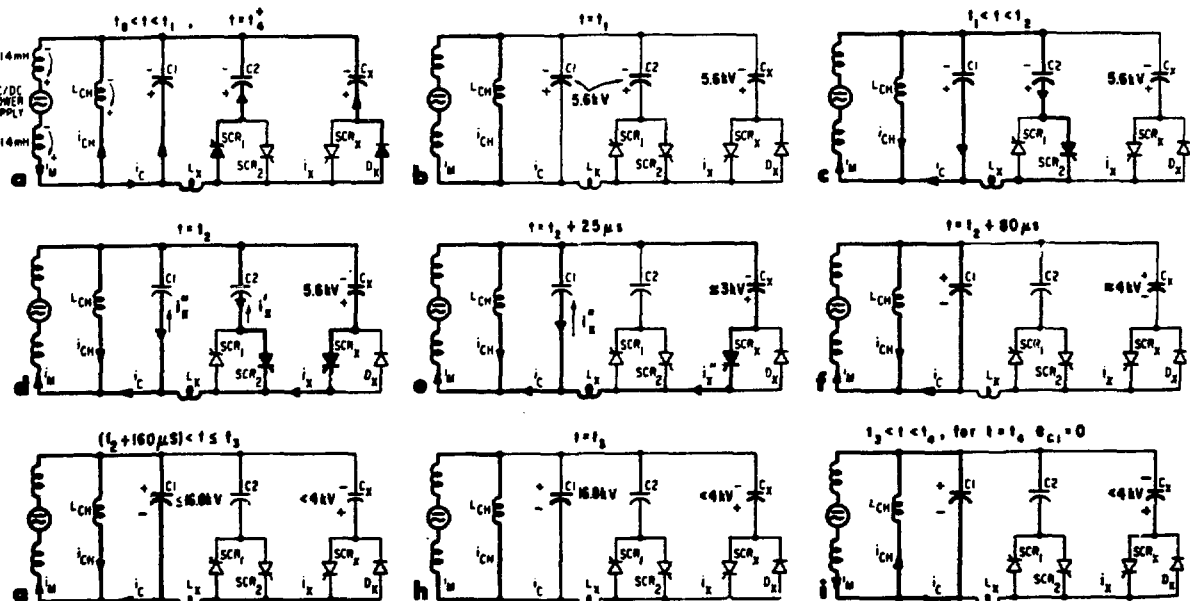


Fig. 4. Block diagram of resonant circuit for 30 Hz acceleration and 90 Hz reset.